Automatic Person Authentication Using Fewer Channel EEG Motor Imagery

By
Orlando X. Nieves Adorno
A thesis submitted in partial fulfillment of the requirements for the degree
of
MASTER OF SCIENCE
in
COMPUTER ENGINEERING
UNIVERSITY OF PUERTO RICO
MAYAGÜEZ CAMPUS
2016

Approved by:

Vidya Manian, Ph.D. President, Graduate Committee	Date
Emmanuel Arzuaga, Ph.D. Member, Graduate Committee	Date
Pedro I. Rivera Vega, Ph.D. Member, Graduate Committee	Date
Omar Colón, Ph.D. Graduate Studies Representative	Date
José G. Colom, Ph.D. Department Chairperson	Date

Abstract of Thesis Presented to the Graduate School
of the University of Puerto Rico in Partial Fulfillment of the
Requirements for the Degree of Master of Science

Automatic Person Authentication Using Fewer Channel EEG Motor Imagery

by

Orlando X. Nieves

Chair: Dr. Vidya Manian
Department: Electrical and Computer Engineering Department

In today's world, there are different aspects of security in which appropriate computing technologies play an essential role. One such aspect is person's identification. While there are numerous ways to identify a person, from using finger prints to using face recognition; most of them exhibit, on one way or the other, unacceptable levels of reliability. On the other hand, recent developments in brain computer interfaces (BCI), using Electroencephalogram (EEG) signals have been emerging as a feasible option for identification systems. Current EEG based authentication systems use more than 8 up to even 60 electrodes placed on the scalp to record data. In this work, we propose and analyze an approach in which person's identification is achieved by measuring the EEG signals that the person generates while imagining simple motor movements, and which requires as few as 2 to 6 channel electrodes. The system uses the Short Time Fourier Transform (STFT) for extraction of time-frequency features also called as spectrogram. Energy, variance, and skewness features are computed on the spectrogram. These features are used to train a support vector machine and a neural network classifier. The classifiers are tested for person authentication with testing data using cross-validation. Results using a different number of channels with optimum features are presented. A Graphical User Interface is also presented for easy use of the person authentication system.

Resumen de tesis presentado a la Escuela Graduada
de la Universidad de Puerto Rico como requisito parcial de los
requerimientos para el grado de Maestría en Ciencias

Autenticación Automática de Persona que Utiliza Menos Sañals de EEG usando Imaginacíon Motriz

por

Orlando X. Nieves

Consejero: Dr. Vidya Manian

Departamento: Ingeniería Eléctrica y Computadoras

En el mundo de hoy, hay diferentes aspectos de seguridad en los cuales la tecnología computacional apropiada juegan un rol esencial. Uno de estos aspectos es el identificar una persona. Hay numerosas maneras de identificar una persona, desde el uso de huellas dactilares a reconocimiento facial; pero la mayoría exhiben, de una manera u otra, niveles inaceptables de confiabilidad. Por otro lado, nuevos avances en interfaces neuronales directas (IND), usando señales de electroencefalograma (EEG en ingles), han empezado a sonar como opciones factibles para sistemas de identificación. Sistemas de identificación actuales que usan EEG, usan mas de 8 y hasta 60 electrodos posicionados en el cuero cabelludo para recolectar información. En este trabajo, proponemos y analizamos un nuevo enfoque en el cual la identificación de una persona se consigue midiendo señales EEG que la persona genera cuando se imaginan movimientos motores simples, y lo cual requiere tan poco como 2 a 6 electrodos. El sistema utiliza Transformada de Fourier de Tiempo Corto (Short-time Fourier transform, STFT) para la extracción de características de tiempo y frecuencias, las cuales se grafican en un espectrograma. Caracteristicas de energía, varianza, y asimetría son computadas en el espectrograma. Estas características se usan para entrenar máquinas de soporte vectorial y un clasificador de redes neuronales.

Los clasificadores se verifican con datos de prueba utilizando validación cruzada. Presentamos resultados utilizando cantidades diferentes de canales con caractersticas óptimas. Una interfaz gráfica de usuario (GUI, en ingles) también es presentada para el uso sencillo del sistema identificador de personas.

I dedicate this to my parents, thanks for helping me get to this point and to every one that suported me.

Acknowledgment

I would like to thank Dra Vydia Manian to make possible this work. I would also like to thankthe assistance of all persons and volunteers whose participation was essential in the successful completion of the work, thanks also to Army Research Laboratory and the U.S. Army Research Office under grant W911NF-13-1-0121. University of Puerto Rico for providing the software platforms for data processing.

Contents

List of Figures

List of Tables

List of Abbreviations

BCI Brain Computer Interface

BR BrainVision Recorder

DFT Discrete Fourier Transform

DNA Deoxyribonucleic acid

EEG Electroencephalogram

GUI Graphic User Interface

NN Neural Network

RBF Radial-Basis Function

ROC Receiver Operating Characteristic

STFT Short-Time Fourier Transform

SVM Support Vector Machine

List of Symbols

GB Gigabyte.

Ghz Frequency (Gigahertz).

Hz Frequency (Hertz).

Khz Frequency (Kilohertz).

min Minutes.

s Seconds.

Chapter 1

INTRODUCTION

1.1 Motivation

Biometrics is the measuring and statistical analysis of people's physical and behavioral attributes. This technology can be used to define an individual's unique identity, often employed for security purposes. The traditional biometric traits are typically based on face recognition, retina or iris scanning, fingerprints, hand geometry, palm print signature, keystroke entry pattern, or voice recognition [1]. However, many of these traits can be forged or stolen. Fingertips, for example, can be damaged by an injury or can be forged by a gummy finger. Face recognition application can be tricked by disguises. Brain waves or Electroencephalogram (EEG) is the electrical activity of an individual's brain that is unique and cannot be tampered with. Hence EEG is proposed as an alternative or an additional way of securing biometric applications [2].

EEG signals are gathered from electrodes that are placed in several locations on the scalp. Because everyone's brain is structured differently, each EEG signal is unique for each person. EGG uniqueness makes the biometric un-forgeable or un-duplicable. The main disadvantage of using EEG signals is the setup for data acquisition. This setup can take up to 15 minutes to complete. This is impractical for an identification system that needs immediate results. There have been a few but not many papers reporting studies on EEG signals as biometrics [2, 3, 4, 5, 6, 7, 8]. Most of them use more than 32 electrodes and have a complicated data acquisition procedure using images or other sensory inputs to stimulate the brain. This process is time-consuming and makes it impractical to implement a real-time biometric system based on EEG. In this thesis work, we propose a simpler identification mechanism that reduces the number of electrodes to 3 and uses simple motor imagery features of the body without compromising the results.

This involves minimal setup time and makes a more practical identification system.

1.2 Outline

The outline of this thesis is as follows. Chapter 2 gives a brief description of the methods and algorithms presented in this document. The step by step process of the completion of the objective is explained in Chapter 3. A study of the results using different channels and classifiers using EEG signals to identify a person are given in Chapter 4. Chapter 5 Ilustrates a sample Graphic User Interface(GUI). Finally, Chapter 6 gives the conclusions and the direction for further development.

1.3 Objective

1.3.1 General Objective

- To develop and implement a person authentication system using brain EEG motor imagery.
- The system will make use of a minimal number of electrodes.
- Implement the system to run in real-time.

1.3.2 Specific Objectives

- Experiment with different numbers of nodes to get maximum identification accuracy.
- Test with SVM and NN so that the authentication system can authenticate an unknown subject in real-time.

Chapter 2

THEORETICAL BACKGROUND

This chapter describes important concepts about EEG signals and the Brian Computer Interface (BCI) system, including the algorithms used for its implementation in this work. We use EEG signals as the input from the users to the system. The input signals are then transformed to time-frequency representation using short-time Fourier transform (STFT). A spectrogram is used as feature extraction method, and classification stage is implemented using Support Vector Machine (SVM) and Neural Network(NN).

2.1 Biometric

Using a person's behavioral or physiological characteristics is refered to as biometric recognition. For a characteristic to be considered for as a barometric, it must be

- **Universal:** It's a characteristic that everyone has.
- **Distinct:** It's a characteristic that differs form each person
- **Permanent:**It's a characteristic that is long lasting.
- **Collectible:** It's a characteristic that can be measured quantitatively

2.1.1 Biometric system

A biometric system uses biometric recognition for personal recognition. For a biometric system to use it has to consider:

- **Performance:** The accuracy and efficiency of a biometric system

- **Ethical** While a biometric system might be good; it might pose ethical problems with users.
- **Circumvention** It should be hard to impossible to fool the system.

2.1.2 Current Biometrics

This section describes some of the current biometric systems employed today, and their disadvantages employed today [12].

- **DNA** Deoxyribonucleic acid (DNA) is blueprint for one's individuality. Except for twins, everyone has a different DNA. While DNA would make it a good use for bioethics, it has some issues.
  1. While it may be unique, it's easy to get a hold of, this makes it susceptible to being impersonated.
  2. A real-time system would be impossible because DNA matching needs chemical methods.
- **Ear:** Using the distance of a landmark location on an ear a salient point on the pinna we can use biometrics to identify a person by their ear.
- **Face Recognition:** Since birth human beings have been able to determine people by their face. Today systems use face recognition to identify mug-shots to identifying a person in a cluster of people. Unfortunately, a system is not safe as a person may change their appearance and the system may not be able to identify them.
- **Facial, hand, and hand vein infrared thermogram:** Using infrared camera we capture the pattern of heat generated by the human body. This biometric system is can be uses for cover identification. While this system does not require contact, in an uncontrolled environments image acquisition is challenging.
- **Fingerprint:** Determined during the first 7 month of fetal development, each human has their own finger print. While this can be an adequate identification system it suffers from minor errors, the first is that they require computation power to be able to identify the person. Other factor like aging and bruises may cause the system to have errors.
- **Gait:** The gait is the way a person walks, while it may not be highly discriminatory it still discriminatory enough to be use for low level security.

- **Hand and finger geometry** By taking the measurements of the human hand, which include the shape size of palm and length and widths of the fingers. This a geometry based verification system has been used commercially around the world. While they are easy to use the geometry of the hand isn't very distinctive and hand information might have to change because of growth for children.

- **Iris:** Formed during fetal development, the visual appearance of the iris develops during the first two years of life. Like fingerprints the iris is unique for each person (not even twins have the same eyes) which makes them perfect for a biometric system. Currently, we still trying to develop a cheap and large-scale biometric system.

- **Keystroke** The way a person write on a keyboard can be considered a biometric system. This biometric system is considered a behavioral biometric. While it may not be unique keys stroke biometrics offer enough discriminatory information to be used as a biometrics.

- **Signature**: Each person has a unique signature, how the person signs his names varies force person to person. While signatures may be hard to forger, there are professionals that can do it which make it not a good identification system.

- **Voice**: Each person's voice is based on the shape and size of the body part that created the voice: vocal tracts, mouth, nasal cavities and lips. While, the body parts mention don't change for an individual, but the person could age, medical condition or emotional state might change the voice. Voice isn't very distinctive, which makes unsuitable for an large -scale identification system.

2.2 EEG Signals

Electroencephalography (EEG) is an electrical activity of an individual's brain that can be collected using electrodes. EGG are created by the electrical communication of millions of neural cells. There are five different frequency band in which EEG can be divided, called brain rhythms these are[13] :

- Delta (δ) rhythms are between (0.5Hz-3.5Hz). There are associated with deep sleep and are common in newborns.

- Theta (θ) rhythms are between (3.5Hz-7.5Hz)); they are most common during sleep. This can be seen in infants and children but high θ rhythms on an awake adult it is a sign of a brain disorder.
- Alpha (α) rhythms are between (7.5Hz-12.5Hz) under mental inactivity and relaxation, best seen with eyes closed.
- Beta (β) rhythms are between (12.5Hz-30.5Hz) of less amplitude than the α rhythms. During states of tension or anticipation, β rhythms are usually enhanced.

2.3 Spectrogram

The spectral content of the EEG signals is non-stationary, which means the signal changes over time. The Discrete Fourier Transform (DFT) is a mathematical operation that decomposes a waveform into a sum of sinusoid components, where the coefficients represent the correlation between the signal and the particular frequency sinusoid. But applying the DFT, along the signal does not reveal the transitions in the spectra, it just shows the frequencies present. Hence, applying the DFT over short periods of time (regular intervals) known as STFT is used. The EEG signal can be considered as stationary. This approach allows identification of the interval of time at which all frequencies are present in the signal. The discrete STFT is computed using a window function w centered at time n, given as:

$$y(n,k) = \sum_{m=-\infty}^{\infty} x[m]w[n-m]e^{\frac{-j2nkm}{N}} \tag{2.1}$$

where x[m] is the signal to be analyzed and N is the frequency sampling factor. The resulting STFT is represented as a matrix with time and frequency $\omega = 2\pi k \ / \ N$ information. The size of the window has the effect of changing the time-frequency resolution, with a wider window better frequency resolution but lower time resolution, and vice versa for a narrow window are obtained.

2.4 Energy

Energy defined on the STFT could characterize signal complexity with the changes in time, and also many of the characteristics in the frequency domain, which had a good time-frequency local capabilities. Let EHL, EHR be the energy distribution of the spectrogram of imagining left-hand movement and imagine right-hand movement signals yHL and yHR, respectively. They are calculated as below

$$E_{HL} = \frac{1}{n}\sum_{i=1}^{n} y_{HL_i} \tag{2.2}$$

$$E_{HR} = \frac{1}{n}\sum_{i=1}^{n} y_{HR_i} \tag{2.3}$$

The same features are also computed on imagining left foot movement and imagine right foot movement and are given as E_{FL} and E_{FR}.

They have been used widely for face recognition. For EEG signals they are calculated as follows:

$$E_{HL} = \frac{1}{n}\sum_{i=1}^{n} y_{FL_i} \tag{2.4}$$

$$E_{FR} = \frac{1}{n}\sum_{i=1}^{n} y_{FR_i} \tag{2.5}$$

$$E_{T} = \frac{1}{n}\sum_{i=1}^{n} y_{Ti} \tag{2.6}$$

where n is the length of the spectrogram. The same features are also computed on imagining left-foot movement and right-foot movement and are given as E_{FL} and E_{FR}. Another motor imagery task the imagination of tongue movement. The energy feature computed on this signal is E_T. The energy features are concatenated into a feature vector E for each subject.

$$E = \{E_{HL}, E_{HR}, E_{FL}, E_{FR}, E_T\} \tag{2.7}$$

2.5 Standard Deviation

The standard deviation of vector L is defined as

$$SD = \sqrt{\frac{1}{N-1}\sum_{i=1}^{N} |L_i - \mu|^2} \tag{2.8}$$

the μ is defined as the mean.

2.6 Skew

Skew is the measure of the asymmetry of the data around the mean level. It's defined as

$$S = \frac{E(x-\mu)^3}{\sigma^3} \tag{2.9}$$

where μ is the mean of x, σ is the standard deviation of x defined in function 2.8 and E(t) is the expected probability.

2.7 Support Vector Machine

The kernel machine or support vector machine (SVM) is one of the most recent and powerful classifiers there is. It uses a discriminative hyperplane that maximizes the margins, which is the distance between the closest instances to the hyperplane[14]. By maximizing the margins, the SVM selects the accurate hyperplane.

Suppose we have two classes with labels -1/+1

$$min\frac{1}{2}\sum_{i=1}^{n} a_i - \frac{1}{2}\sum_{i=1}^{n}\sum_{j=1}^{n} y_i y_j a_i a_j K(x_j, x_j) \tag{2.10}$$

$$s.t. \sum_{i=1}^{n} y_i a_i = 0, 0 \leq a_i \leq C \tag{2.11}$$

where C is the penalty factor which allows controlling of the trade-off between the misclassification and the size of the margin between classes. Because the SVM uses a hyperplane it would only be able to classify classes that can be separated linearly; the problem has to be transformed to a higher dimension for non-linear problems, this is done with a kernel function.

The SVM can use different kernel functions or kernel tricks, the most used are linear, polynomial, radial-basis function(RBF), and sigmoid. Let x be the training vector then the linear kernel would be:

$$K(x_i, x_j) = x_i^t x_j \tag{2.12}$$

The polynomial kernel:

$$K(x_i, x_j) = (\gamma x_i^t x_j + r)^q, \gamma > 0 \tag{2.13}$$

The RBF kernel:

$$K(x_i, x_j) = exp(-\gamma \|x_i - x_j\|^2), \gamma > 0) \tag{2.14}$$

The sigmoid

$$K(x_i, x_j) = tanh(\gamma x_i^t x_j + r) \tag{2.15}$$

where q, r and γ are set by the user[15].

While the kernel function helps with the non-separable classes, SVM is still not a multi-class classifier. In other words to make the SVM a muti-class classifier several algorithms have been developed: one-versus-one and one-versus-all are the most popular.

For this research, the LIBSVM library that's being used uses one-verseone[15]. Unlike the one-versus-all algorithm that makes n models for n classes one-verses-one makes model one for every pair of classes. While one-verses-one has more models it has been tested to be better with larger problems[16, 23].

2.8 Neural Network

The Multilayer Perceptron or Neural Network(NN) were designed after studying the brain. An abstract mathematical model representation of a neuron was design by McCulloch and Pi tts[McChulloch]. Their model

- receives as input a finite number $x_1, x_2, \ldots, x_n$
- it calculates the sum $s = \sum_{i=1}^{m} w_i x_i$ of the weights $w_1, \ldots, w_m$
- uses a threshold on the result s and outputs 0 or 1 depending on the value

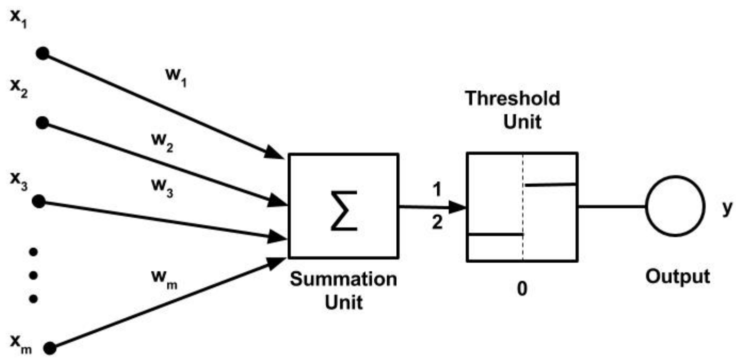

Fig 2.1: The McCulloch-pit Model of the neuron

The MccCulloch model outputs 1 if

$$w_1x_1 + w_2x_2 + \cdots + w_mx_m > T \tag{2.16}$$

or 0 otherwise. The model described in figure 2.1 can be rewritten as

$$D = w_0x_0 + w_1x_1 + \cdots + w_mx_m \tag{2.17}$$

where the output will be 1 if $D > 0$ and output 0 if $D \leq$ and where w_0 is the bias weight. This new model is represented in figure 2.2

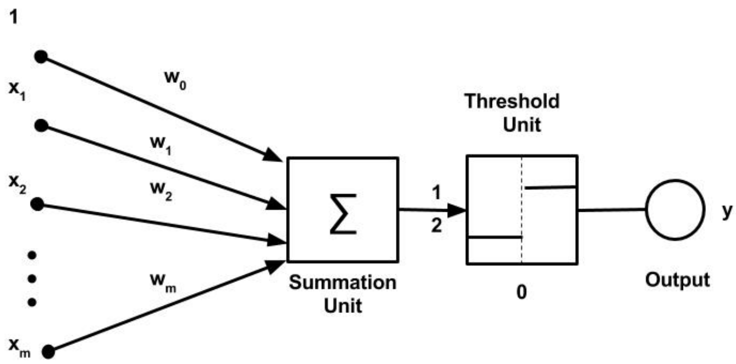

Fig 2.2: Baised weight model

Rosenblatt used the McCulloch model described in figure 2.1 to form a trainable classifier called a perceptron. The perceptron works by giving each input a weight. Theses weight are randomized at first but with each iteration of the data, change to get a better output. A simple example would be:

$$y = \sum_{j=1}^{d} w_j x_j + w_0 \tag{2.18}$$

where w_0 is a weight that comes from a bias unit, w_j is the weight for each value of the vector.

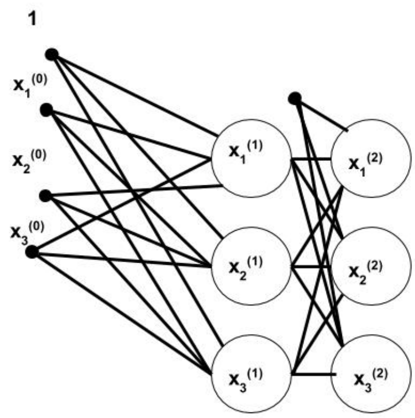

Fig 2.3: A three-layer NN where the weight between $x_i^{(k-1)}$ and $x_j^{(k)}$ is $w_{ij}^{(k)}$

Figure 3.8 shows a three layer NN with nodes $x_1^{(0)}, x_2^{(0)}, x_3^{(0)}$ are the inputs layer and $x_1^{(2)}, x_2^{(2)}, x_3^{(2)}$ are the output layer. The layer in between the input layer and the output layer is called the hidden layer and this can be composed of a multitude of layer and nodes. Having a hidden layer allows an NN to classify classes that are not convex or separated by a hyperplane [17].

2.8.1 Back-Propagation Algorithm

While each weight in an NN starts off randomly, in each iteration of training the weights change try to get the desired target. This change in the weights can't be a small change because it will usually not affect the output of the network. The output of a node would change if the weight changed enough for the sign of that node to change. The back-propagation algorithm changes the weights of the nodes enough for the output to change.

The back-propagation algorithm is composed of two main steps:

1. the feed-forward step

2. back-propagation step

The feed-forward step is composed of calculating the outputs of the nodes starting at layer 1 and working forward to the output layer. While in the back-propagation step the weights are updated in an attempt to get better agreement between the output of the NN and the target output.

The back-propagation algorithm contains the fallowing steps [17]:

1. Weights $w_{ij}^{(k)}$ are randomly initialized to a small value, an a constant positive integer is chosen for c.

2. Set $x_1^{(0)}, \ldots, x_{M_0}^{(0)}$ to the features of samples 1 to N .

3. Feed-forward step. For k=0, $\ldots, K-1$ where K is the number of layers in an NN compute

$$x_j^{(k+1)} = R\Big(\sum_{i=1}^{M_k} w_{ij}^{(k+1)} x_i^{(k)}\Big), \tag{2.19}$$

   for nodes j $= 1, \ldots, M_{k+1}$. For the threshold, the sigmoid function was used

$$R(s) = \frac{1}{(1+e^{-s})}. \tag{2.20}$$

4. Back-propagation step. For the nodes in the output layer, j$= 1, \ldots, M_K$ compute

$$\delta_j^{(K)} = x_j^{(K)}(1 - x_j^{(K)})(x_j^{(K)} - d_j). \tag{2.21}$$

   For layers k $= K-1, \ldots, 1$ calculate

$$\delta_i^{(k)} = (1 - x_i^{(k)}) \sum_{j=1}^{M_{k+1}} \delta_j^{(k+1)} w_{ij}^{(k+1)} \tag{2.22}$$

   for $i = 1, \ldots, M_k$.

5. Replace $w_{ij}^{(k)}$ by $w_{ij}^{(k)} - c\delta_j^{(k)} x_i^{(k-1)}$ for all i,j,k

6. Until $w_{ij}^{(k)}$cease to change significantly, repeat steps from 2 to 5.

Chapter 3

METHODOLOGY

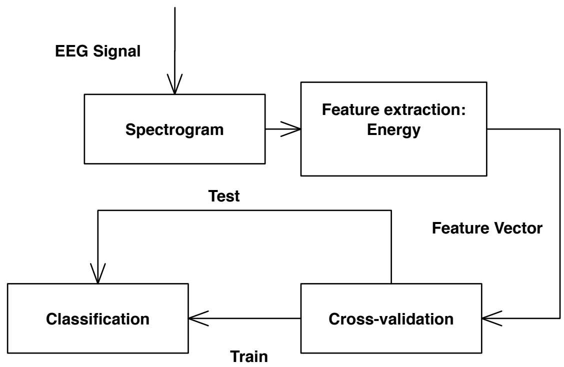

Fig 3.1: Flow chart of the methodology.

The methodology consists of EEG data acquisition for the motor imagery tasks of thinking movement in five parts of the body such as left hand, right hand, left foot, right foot and tongue. Once sufficient trials of EEG signals for the above tasks are obtained from a subject, the spectrogram is computed on each of these signals. The feature extraction stage consists of computing the energy features on the spectrogram. The work flow for the methodology is given in the Figure 3.1.

3.1 Signal acquisition

The EEG signal generated by the cerebral cortex is measured with a different number of active electrodes (maximum 32 possibles) in the scalp surface with AgCl conductive paste applied on the region to provide good conduction. Each subject is seated in a comfortable chair and asked to see the monitor. On the monitor the words left, right, and up are displayed. For the first 120 trials, the subject is told to imagine moving his left and right hand based on the word in the monitor. The next 120 trials the subjects will be told to imagine moving their left and the right leg based one the word in the monitor, and for the last 60 trials the subject is told to imagine moving their tongue up. The voltage recorded from the scalp is sampled at 500Hz.

3.1.1 Hardware

The hardware used to collect data is composed of: BrainAmp amplifier and Easycap wore on the head. from Brain products. Easycap is an EEG recording device, the device uses 32 ring-shaped electrode to collect 32 channels of data. In Fig3.2 the electrodes can be seen as three colors: white, blue and black. White are the 32 channels electrodes, while blue and black are the reference electrode and black are the ground electrode.

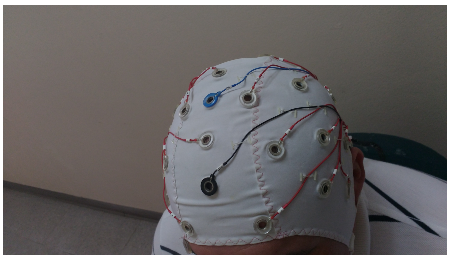

Fig 3.2: Picture of Easycap

The data collected from the Easycap is transmitted to the BrainAmp, which amplifies and digitize the EEG bio-signals collected by the Easycap, see Fig 3.3. The BrainAmp can convert from a sequential 16bit to digital, with a 5 Khz sample per channel.The specifications for the BrainAMp are in table 3.1.

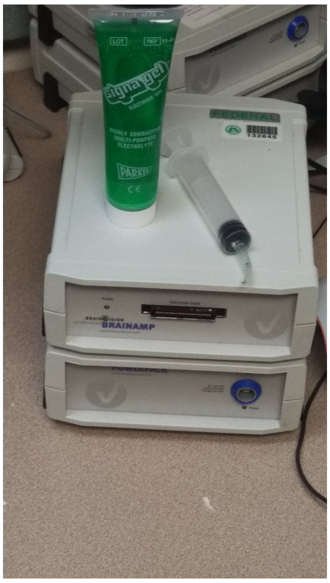

Fig 3.3: Picture of BrainAMp amplifier

Table 3.1: BrainAmps Specifications

Specification	Value
Number of channels	32
Channel type	One electrode as reference
Impute impedance	10MΩ
input noise	$\leq 2\mu v_{pp}$
common-mode rejection (CMR)	$\geq$ 90dB
low-cutoff (high-pass)	0.016 Hz/10s
High-cutoff frequency (low-pass)	1000hz
Measuring range	$\pm$ 3.28mV
Sampling rate	5000 HZ per channel
DC offset tolerance	$\pm$ 300mV
Resolution	0.1 μV per bit
power consumption	Max. 110 ma

The electrode gel shown in fig 3.3 was used to reduce the impedance of the electrodes in the cap to obtain more accurate data. The gel is applied to every electrode in the cap, while the subject is wearing it.

3.1.2 Nodes Location

To improve on former work, data was collected using a different number of channels. Using only groups of electrodes of sizes 2, 3,4,6, and 8 was the data used fro the experiment. The nodes that were used are listed below:

1. *C3, C4*
2. *C3, Cz, C4*
3. *F3, Fz, F4*
4. *O1, O2, Pz*
5. *C3, C4, FC5, FC6*
6. *C3, C4, FC1, FC2, FC5, FC6*
7. *C3, C4, F3, F4, FC1, FC2, FC5, FC6*

This group was chosen based on previous work[18], where they used 2 electrodes for each channel. The work mention uses 8 electrodes for EEG data, where channel 1 corresponds to FC4 and CP6, corresponds to 2 was P2 and P6, channel 3 corresponds to FC3 and CP3, and channel 4 corresponds to P5 and P1.

The locations of the channel are displayed in Figure 3.4. The first two channels, channels C3 and C4 were selected to try and improve the time required to set up the biometric system without compromising too much on the results. Channels C3, Cz, and C4 were selected to improve results on the first channels selected without compromising too much on time. Because of their proximity to the reference node channels F3, Fz, and F4 were selected. Channels O1, O2, Pz were selected because of the visual part of the brain is located in the same area. To improve on results [18] channels C3, C4, FC5, and FC6 were selected. Channels C3, C4, FC1, FC2, FC5, and FC6 were selected to try to improve the

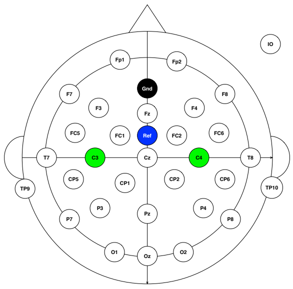

(a) Group 1: C3, Cz, C4

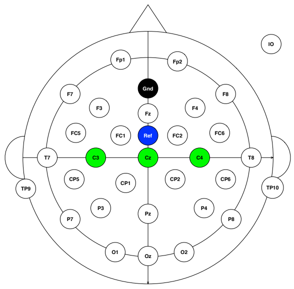

(b) Group2: F3, Fz, F4

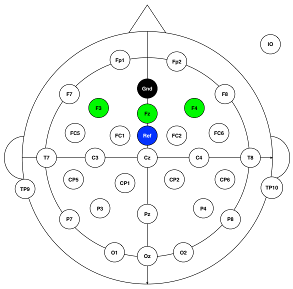

(c) Software right display

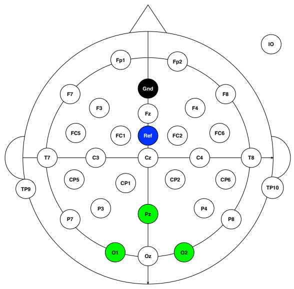

(d) Software right display

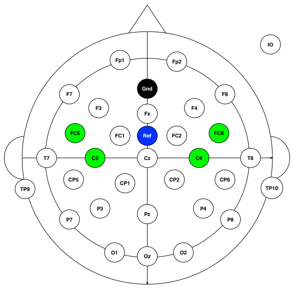

(e) Software right display

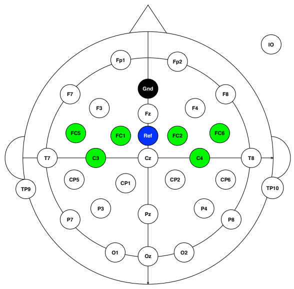

(f) Software right display

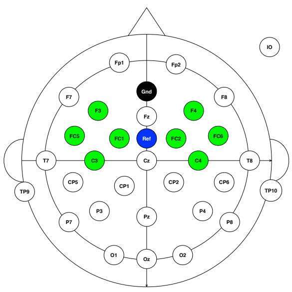

(g) Software right display

Fig 3.4: Position of electrodes in Easycap illustration

3.1.3 Software

(a) Software right display

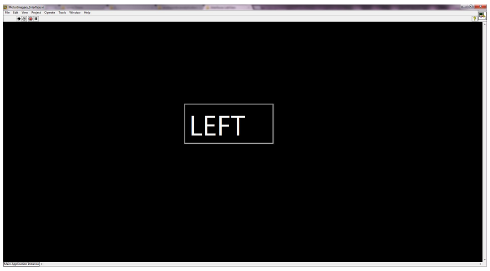

(b) Software left display

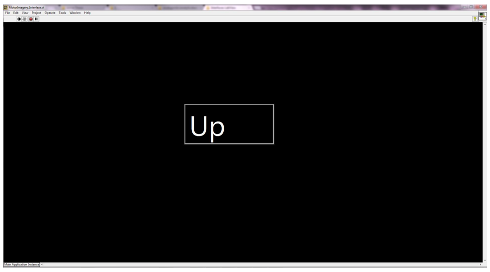

(c) Software up Image

Fig 3.5: Images of the software that each subject saw.

A graphic user interface(GUI) was created using labview to display the commands to the subject. The GUI displays the words: Right, Left and Up to the subject. Fig 3.5 is what the subject sees in the computer monitor. This work is similar to the work done in[19], where the electrodes used are C3,C4

Besides showing the words, the GUI also sets the time stamps for each label in the EEG data that was being collected. The software that was used to collect EEG data was the BrainVision Recorder (BR). The BR is a flexible recorder that records and shows in real time, the EEG signal being collected by the Easycap. The data recorded by the BR is stored in the computer as raw digitized data. An example of the EEG data can be seen in Figure 3.6.

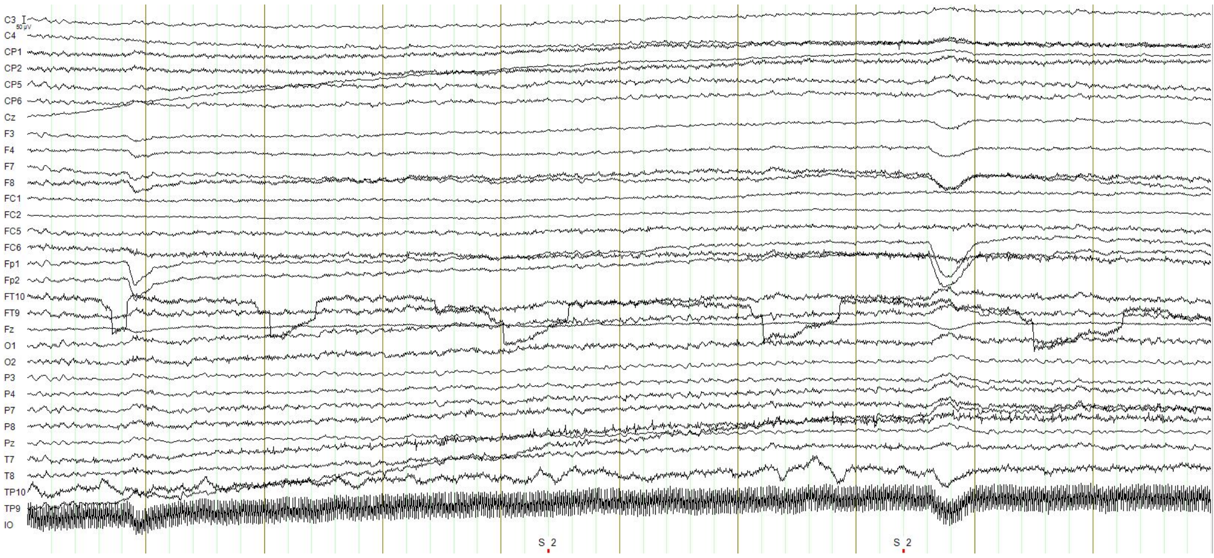

Fig 3.6: BR display where the leters and symbols on the left hand side are the 32 channels and the read line in the buttom are the time tags.

After recording the data with BR, an application called BrainVision Analyzer is used to create generic data out of the data recorded.

3.2 Feature extraction

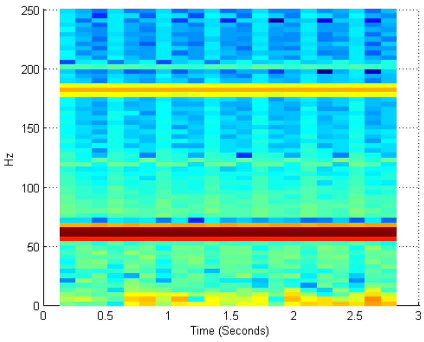

(a) Spectrogram of right hand data

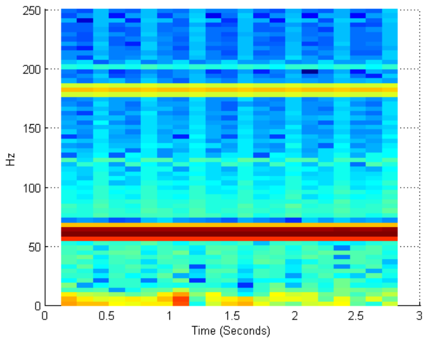

(b) Spectrogram of left hand data

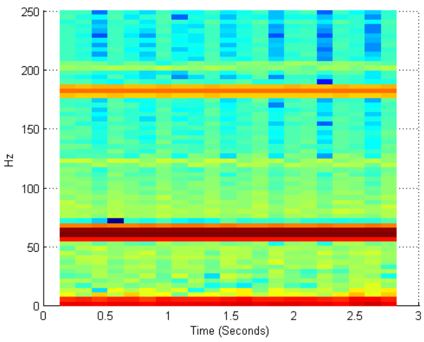

(c) Spectrogram of right leg data

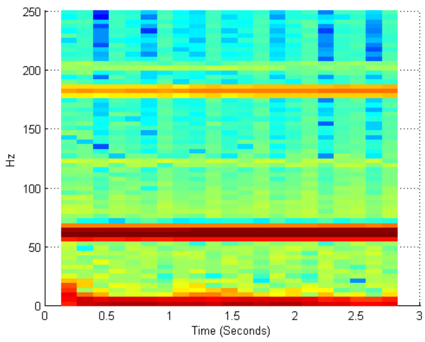

(d) Spectrogram of left leg data

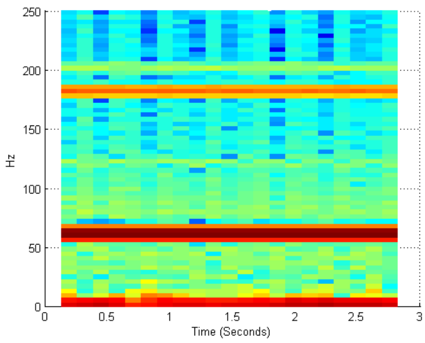

(e) Spectrogram of tongue data

Fig 3.7: Spectrogram for data of first subject .

After the data is collected and the generic data has been acquired, the spectrogram function of matlab is used to get the STFT of each of the EEG sample. Figure 3.7 shows the spectrogram of the first subject. STFT is done similar to [20] where the window function is being multiplied by the Fourier Transform of the EEG. After getting STFT of each feature, the STFT multiplied by $10log_{10}$, this is done to get the decibel value which the first 5 observations. The next 2 observation are the skew and the variance of the STFT of each EEG sample. This makes 15 observations for each channel.

3.3 Feature Selection

To quantify the separation between classes, this research used the same procedure in [21]. Let M be the normalized matrix of the features and $\hat{\mathrm{Y}}$ is the feature matrix for each subject. We then can get the sum of the distance:

$$D_L = \sum_{J} |\hat{Y}_{i,j} - M_i| \tag{3.1}$$

where i is the feature index , L is the number of the feature's, j is the class index, and J is the total number of matrix imagery class. We also calculate the standard deviation for each feature :

$$\sigma_L = \sqrt{\frac{1}{J}\sum_{j=i}^{J}(Y_{i,j} - M_i)^2} \tag{3.2}$$

Sorting the results of equation (3.1)-(3.2), the first 60 features were selected. Those were the features that are used for classification.

3.4 Cross-validation

After selecting the best features from the selected channels, the data was split using 10 Kfold partitions, this done for cross-validation. Cross-validation is use to get accurate accuracy for the classifier C. Accuracy is defined here as: $\mathbf{Acc} = \mathbf{Pr}(\mathbf{C}(\mathrm{v}) = \mathrm{y})$ for a randomly selected instance $\langle v, y\rangle \in X$, where the probability distribution over the instance space is the same as the distribution that was used to select instance for the inducer's training set. Where the inducer builds a classifier from a given dataset. One accuracy doesn't give many details about the classified data,that's why cross-validation is used.

The function used in this experiment is the k-fold cross validation. In k-fold cross-validation (the folds) $D_1, D_2, \ldots D_k$ are randomly split k subset of approximately equal size o f data set D. For each of the k subset, the inducer is trained and tested k times, where each $t \in /1, 2, \ldots, k/$, it is trained on $D \setminus D_t$. Let the instance $x_i = \langle v, y \rangle$ be a test set in $D_(i)$ then the cross-validation estimate of accuracy:

$$acc_{cv} = \frac{1}{n} \sum_{\langle v_i, y_i \rangle \in D} \delta(I(D \setminus D_{(i)}, v_i), y_i) \tag{3.3}$$

where $\delta(i, j) = 1$ if $i = j$ and 0 otherwise and I is the inducer. Then a complete cross-validation is used where the average of all $\binom{m}{m \setminus k}$ possibilities for choosing $m \setminus k$ instance out of m[22].

3.5 Classification

After using the 10 KFold partition to divide the data into training and testing set,the data was run through two different classifiers, the (SVM) and the (NN).

3.5.1 Support Vector Machine

As discussed in section 2.7 this experiment used LIBsvm code for the SVM. The kernel that was used is the Polynomial kernel, because the Polynomial maps the input to a higher dimensional space and with more subject it's easier to classify. The SVM uses a one versus one system in this case its makes a model for each class and compares with each and gives a point to the class that won, whichever class has the most points the data is assigned that label.

3.5.2 Neural Network

For this experiment matlab, NN toolbox was used. The toolbox uses different types of training function, for this experiment trainscg function was used to train the NN . The trainscg The NN that was used in this experiment had 2 hidden layers one with 41 nodes and the second with 22 nodes. Fig 3.8 is an illustration of the NN that was used in this experiment, where the input layer has 60 nodes and the output layer were 20 nodes.

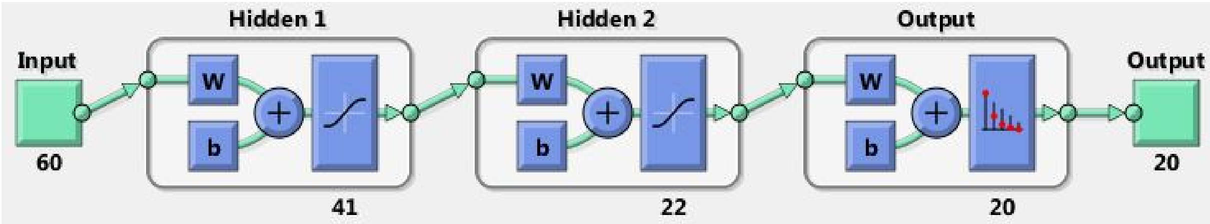

Fig 3.8: Matlab Image of NN

3.6 Experiment

Each subject was told to sit in a chair and to think of moving either their hands, feet or tongue based on the software described in section 3.1.3. The first 60 trials the subject was asked to think about moving his or her hands while the display showed left and right. The next 60 trials were the same except that the subject had to think that he or she was moving their legs. For the final 60 trials, the subject was asked to think they were moving their tongue up. The experiment is composed of 20 different subjects between the ages of 18-28 both female and male. After the data collection was complete, time-frequency representation and features were extracted from SFTF. After the data was randomly partitioned the classifiers were trained. Using different channels to compare the results of each of the classifiers. After 6 month data was collected and classfied, from 3 subjects from the 20 subjects to show that the data is constent.

3.7 Time Consumption

Table 3.2: Time Table

Operation	Time Consumed
Data Separation	9:21min
Feature Extraction	6:30min
Feature Selection	1.5s
SVM Training Time	20s
SVM Predicting time	1.4s
NN Training Time	5:40in
NN Predicting Time	1.5 s

As mentioned on section 2.1.1, a biometric system has to be both accurate and efficient, this is why efficiency has to be considered as much accuracy. Table 3.2 shows the time consumption for each of the procedures mentioned in last sections. The table shows that

Data Separation is 9:21min. This time is how long the system took to load all 20 subjects' raw data into the system. Feature Extraction takes 6:30 min because of all the data that has to be used. These two high times only happen once, the first time is ran. The table also shows that the SVM classifier is faster than the NN. The computer that was used had a Intel Xeon 2.6 Ghz dual core and a 32 GB RAM

Chapter 4

RESULTS

In this chapter, classification accuracy for different subjects is presented. The accuracy include the use of 2, 3, 4, 6, and 8 channels and SVM, NN classifiers. The data was divided, and 1/10 of the trials were selected for testing. In other words, 6 trials were randomly chosen out of the 60 trials, ten times. After the feature extraction and the feature selection, the data was left with a feature matrix of 60 rows with 132 columns, for each subject. Multiplying the 132 columns by the ten folds that were done, there are 1320 observations for each subject. The results for these instances are recorded in the confusion matrices and the receiver operating characteristic (ROC) curve. These results are from pre-recorded data and not real time data.

The confusion matrix shows the results for each subject by showing how many of the 1300 observations were correctly classified. The last column of the confusion matrix shows the percent of all observations that were correct; this gives the accuracy of the classifier. The final row in the confusion matrix shows the parentage of observation that was classified correctly out of all the observation that were classified as the subject.

The ROC curve is a plot that shows all the pairs of true-positives and true-negatives, varying the decision threshold over all the results observed. In ROC curve the y-axis is defined as (number of true-positive test results)/(number of number of true positives + number of false-negative test results), while x- axis is defined as (number of false-positives test results)/(number of number of true-negative + number of false positive test results). The area under the ROC is usually used to compare classifiers, the closer to 1 the area, the better the classifier. [33]. Because the ROC curve is supposed to be done for binary classification a one-vs-all method was used.

4.1 Channels: C3, C4

Table 4.1 shows the confusion matrix of the SVM classifier for the channels C3 and C4. While most of the accuracy in the matrix are above 80%, subject S6 and S10 accuracy are below 80%. S1 has a total of 91.21% positives, of all the data classified as S1 only 85.57% were accurate. 66 of S18's data got classified as S1 which decreased the accuracy of S1. The data of S6 wasn't classified well and got 78.11% accuracy, while many of the other data were classified as S6 and lowered the outputs average to 68.14%. The table shows that the average for all the data is 91.41%.

Table 4.1: SVM Confusion Matrix for Channels C3, C4

		Outputs																				
		S1	S2	S3	S4	S5	S6	S7	S8	S9	S10	S11	S12	S13	S14	S15	S16	S17	S18	S19	S20	
Targets	S1	1204	0	0	0	0	5	13	5	0	10	0	4	0	27	4	0	0	48	0	0	91.21%
	S2	0	1268	0	0	0	13	0	0	0	13	0	24	0	0	0	0	0	2	0	0	96.06%
	S3	0	0	1313	0	0	0	0	0	1	0	4	0	0	0	1	1	0	0	0	0	99.47%
	S4	1	0	0	1315	0	0	0	0	0	0	0	0	0	0	0	0	0	4	0	0	99.62%
	S5	2	0	0	0	1303	3	0	0	4	0	7	0	0	0	0	1	0	0	0	0	98.71%
	S6	2	26	1	0	2	1031	0	35	0	77	34	66	26	0	15	0	3	1	0	1	78.11%
	S7	16	0	0	0	0	0	1297	1	0	5	0	0	0	0	0	0	1	0	0	0	98.26%
	S8	5	0	0	0	0	61	1	1133	0	17	26	3	8	1	41	6	4	6	0	8	85.83%
	S9	0	0	4	0	0	0	0	0	1313	0	0	0	0	0	0	3	0	0	0	0	99.47%
	S10	19	19	0	0	0	142	4	40	0	1013	4	17	15	0	3	0	26	18	0	0	76.74%
	S11	0	0	4	0	12	52	0	10	0	1	1234	1	6	0	0	0	0	0	0	0	93.48%
	S12	10	6	0	0	0	99	0	9	0	19	22	1060	11	0	66	0	1	13	0	4	80.3%
	S13	12	0	0	0	0	36	0	22	0	17	2	21	1177	0	0	0	2	19	0	12	89.17%
	S14	62	0	0	0	0	0	6	0	0	0	0	0	0	1251	0	0	0	1	0	0	94.77%
	S15	6	1	4	0	1	38	0	33	0	0	1	85	2	1	1125	0	0	1	0	22	85.23%
	S16	0	1	0	0	0	0	0	6	0	0	11	4	0	0	0	1281	0	0	17	0	97.05%
	S17	0	0	0	0	0	8	4	21	0	69	0	0	2	1	0	0	1212	0	0	3	91.82%
	S18	66	9	0	6	0	10	0	21	0	25	0	20	21	2	0	0	1	1138	0	1	86.21%
	S19	0	0	0	0	0	0	0	0	1	0	0	0	0	0	0	0	0	0	1319	0	99.92%
	S20	2	0	0	0	0	15	1	32	0	1	3	5	68	0	43	0	5	1	0	1144	86.67%
		85.57%	95.34%	99.02%	99.55%	98.86%	68.14%	97.81%	82.82%	99.55%	79.95%	91.54%	80.92%	88.1%	97.51%	86.67%	99.15%	96.57%	90.89%	98.73%	95.73%	91.41%

Fig 4.1 shows the ROC curve for the data of channels C3, C4. The ROC table shows that most of the subject have a high true positive rate. S6 has the lowest true positive rate, followed by S10, S12 and S19 have the highest true positive rate, while S19 has the highest true positive rate.

Table 4.2 shows the area under the ROC curve. The highest area under the ROC curve is off subject S19, while the lowest was S6.

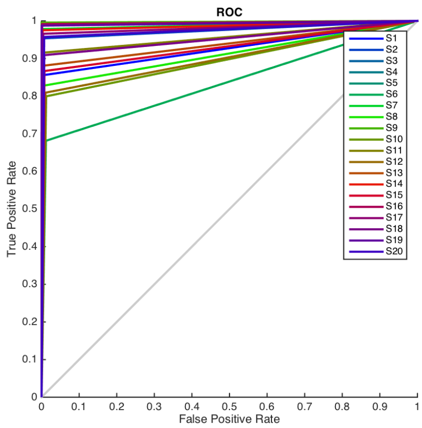

Fig 4.1: ROC figure for SVM for Channels C3 and C4

Table 4.2: ROC Area Under Curve for SVM for Channels C3 and C4

Subject	Area	Subject	Area
S1	0.952	S11	0.965
S2	0.979	S12	0.897
S3	0.997	S13	0.943
S4	0.998	S14	0.973
S5	0.993	S15	0.923
S6	0.881	S16	0.985
S7	0.991	S17	0.958
S8	0.924	S18	0.929
S9	0.997	S19	0.999
S10	0.879	S20	0.932
Average			0.95475

The NN classifier results are shown in Table 4.3, with the average accuracy being 85.91%. The subject with the lowest accuracy was subjec S5 with an accuracy of 10.0%, while the subject with the highest accuracy was subject S19 with an accuracy of 99.39%. Many of the subjects data got miss-classified as S6, which explains why only 68.24% of all the data classified as S6 was correctly classified. S8 is another example of miss-classification, were all the data miss-classified as S8 with an accuracy of 79.41%.

The ROC curve is shown in Figure 4.2, while the area of this ROC curve is on Table 4.4. The highest area for all the subject would be S19, while the lowest area under the curve was off subject S16.

Comparing the results of S5 in Table 4.3 with Table 4.1, on the latter S5 received 98.94%, while on the former S5 only got a 57.5 %. The same outcome appears on S16 where the accuracy in Table 4.1 is 98.18% while in Table 4.3 it is 48.18%. S16 has the lowest accuracy in Table 4.1 while S6 has the lowest accuracy on Table 4.3. The average accuracy of Table 4.3 is 85.19% which is lower than the accuracy of 4.1. The comparison between 4.2 and 4.1 shows the difference between the two classifiers. Comparing the results of the subjects in Table 4.2 with Table 4.4, it can be seen that S19 was the highest area in both tables, while the lowest area changed in both table. Based on the average in both table, SVM classifier was better with an accuracy 0.95475, than NN for this group of channels with a 0.9258.

Table 4.3: NN Confusion Matrix for Channels C3, C4

		Outputs																				
		S1	S2	S3	S4	S5	S6	S7	S8	S9	S10	S11	S12	S13	S14	S15	S16	S17	S18	S19	S20	
Targets	S1	1225	1	0	1	0	0	9	7	0	5	0	11	2	14	2	0	2	40	0	1	92.8%
	S2	0	1265	0	0	0	13	0	0	0	7	4	13	1	0	3	0	1	13	0	0	95.83%
	S3	0	0	1298	0	0	0	0	1	8	1	7	0	0	0	4	0	1	0	0	0	98.33%
	S4	1	0	0	1308	0	0	0	0	0	1	0	0	0	0	0	0	0	10	0	0	99.09%
	S5	0	80	151	0	132	57	91	79	196	71	101	64	0	87	46	67	0	0	96	2	10.0%
	S6	0	36	3	1	0	956	0	31	0	71	45	114	25	0	28	0	5	0	0	5	72.42%
	S7	11	0	0	0	0	0	1293	0	0	5	0	0	1	6	0	0	2	1	0	1	97.95%
	S8	6	0	3	0	1	26	6	1116	0	23	10	3	31	0	56	11	7	3	0	18	84.55%
	S9	0	1	4	0	0	0	0	1	1299	0	1	1	0	0	2	5	0	0	6	0	98.41%
	S10	9	11	2	0	0	106	6	11	0	1024	4	24	38	0	5	0	53	27	0	0	77.58%
	S11	0	0	4	0	0	61	0	13	4	4	1216	6	5	0	0	5	0	0	0	2	92.12%
	S12	8	5	1	0	0	71	0	0	0	23	15	1069	11	0	94	7	1	12	0	3	80.98%
	S13	9	1	0	0	0	21	0	9	0	35	1	38	1155	1	2	0	5	14	0	29	87.5%
	S14	42	1	0	0	0	0	2	0	0	0	0	0	0	1262	10	0	0	3	0	0	95.61%
	S15	5	2	10	0	0	33	0	17	1	2	0	72	3	0	1164	0	0	0	0	11	88.18%
	S16	0	0	2	0	0	2	0	7	12	0	12	2	0	0	2	1277	0	0	2	2	96.74%
	S17	0	0	0	0	0	11	2	1	0	52	0	2	6	1	0	0	1235	7	0	3	93.56%
	S18	83	20	0	62	6	4	20	16	0	34	6	47	60	8	12	0	1	934	0	7	70.76%
	S19	0	0	0	0	0	2	0	0	2	0	0	1	2	0	1	0	0	0	1312	0	99.39%
	S20	5	4	0	0	0	13	0	31	0	1	1	9	71	0	27	1	10	8	0	1139	86.29%
		82.24%	83.1%	82.31%	88.89%	55.49%	66.2%	84.69%	78.44%	80.11%	71.16%	80.29%	68.66%	77.05%	85.47%	75.36%	86.74%	87.0%	80.32%	86.62%	86.37%	85.91%

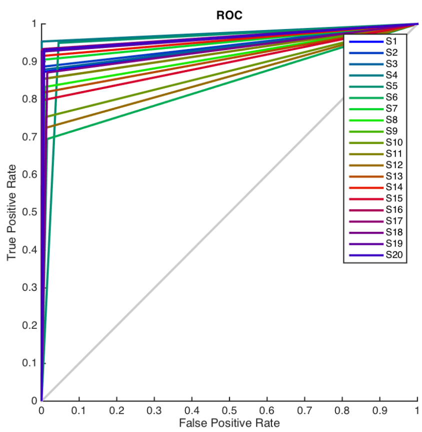

Fig 4.2: ROC figure for NN for channels C3, C4

Table 4.4: ROC Area Under Curve for NN for channels C3 and C4

Subject	Area	Subject	Area
S1	0.96	S11	0.956
S2	0.976	S12	0.897
S3	0.988	S13	0.932
S4	0.994	S14	0.976
S5	0.55	S15	0.935
S6	0.854	S16	0.982
S7	0.987	S17	0.966
S8	0.918	S18	0.851
S9	0.988	S19	0.995
S10	0.881	S20	0.93
Average			0.9258

4.2 Channels: C3, Cz, C4

Channels C3, Cz, and C4 were used to get the results in Table 4.5. S19 had the highest true positive results, while S12 had the lowest. The overall accuracy was 96.19%, most of the accuracy were above 80% except for S19. The confusion matrix also shows that many of the data on S12 got classified as S6, which increased the the false positive percentage of S6.

The ROC curve in Fig 4.3 shows how close the results are for channels: C3, Cz, and C4. The areas of the ROC curve for the SVM classifier are in Table 4.6. The highest area in the table is from subject S19, while the lowest is subject S12. The average Area for the SVM classifier was 0.9799.

Table 4.5: SVM Confusion Matrix for Channels: C3, C4, and Cz

		Outputs																				
		S1	S2	S3	S4	S5	S6	S7	S8	S9	S10	S11	S12	S13	S14	S15	S16	S17	S18	S19	P20	
Targets	S1	1245	0	0	1	0	1	27	2	0	0	0	2	0	0	2	0	0	39	0	1	94.32%
	S2	0	1315	0	0	0	0	0	0	0	0	0	2	0	0	3	0	0	0	0	0	99.62%
	S3	0	0	1315	0	0	0	0	0	0	0	1	0	3	0	0	1	0	0	0	0	99.62%
	S4	1	0	0	1317	0	0	0	0	0	0	0	0	0	0	0	0	0	2	0	0	99.77%
	S5	0	0	0	0	1310	7	0	0	0	0	1	1	0	0	0	0	0	0	1	0	99.24%
	S6	2	1	0	0	1	1199	0	21	0	0	11	57	0	0	19	0	4	5	0	0	90.83%
	S7	31	0	0	0	0	1	1286	0	0	0	0	0	0	0	0	0	0	2	0	0	97.42%
	S8	1	0	0	0	1	37	2	1235	0	0	15	6	0	0	13	0	0	8	0	2	93.56%
	S9	0	0	0	0	0	0	0	0	1318	0	0	0	0	0	0	0	0	0	2	0	99.85%
	S10	0	9	0	0	0	2	0	0	0	1305	0	0	0	0	0	0	4	0	0	0	98.86%
	S11	0	0	0	0	3	10	0	19	0	0	1286	0	0	0	0	0	0	0	0	2	97.42%
	S12	4	2	0	0	1	68	0	19	0	1	1	1128	0	0	81	0	13	2	0	0	85.45%
	S13	0	0	1	0	0	0	0	0	0	0	0	0	1319	0	0	0	0	0	0	0	99.92%
	S14	0	0	0	0	0	0	0	0	0	0	0	0	0	1320	0	0	0	0	0	0	100.0%
	S15	0	1	0	0	1	36	0	5	0	0	0	119	0	0	1158	0	0	0	0	0	87.73%
	S16	0	0	10	0	0	0	0	0	0	0	2	0	0	0	0	1303	0	0	5	0	98.71%
	S17	1	0	0	0	0	19	0	1	0	4	0	13	0	0	3	0	1279	0	0	0	96.89%
	S18	49	0	0	3	0	32	5	17	0	0	0	12	0	0	3	0	0	1195	0	4	90.53%
	S19	0	0	0	0	0	0	0	0	0	0	0	0	0	0	0	0	0	0	1320	0	100.0%
	S20	8	0	0	0	0	23	0	15	0	3	6	9	4	0	7	0	0	4	0	1241	94.02%
		92.77%	99.02%	99.17%	99.7%	99.47%	83.55%	97.42%	92.58%	100.0%	99.39%	97.2%	83.62%	99.47%	100.0%	89.84%	99.92%	98.38%	95.07%	99.4%	99.28%	96.19%

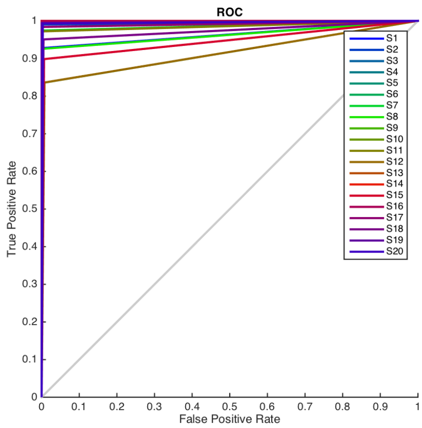

Fig 4.3: ROC figure for SVM for channels C3, C4, and Cz

Table 4.6: ROC Area Under Curve for SVM for Channels C3, Cz, and C4

Subject	Area	Subject	Area
S1	0.97	S11	0.986
S2	0.998	S12	0.923
S3	0.998	S13	0.999
S4	0.999	S14	1.0
S5	0.996	S15	0.936
S6	0.949	S16	0.994
S7	0.986	S17	0.984
S8	0.966	S18	0.951
S9	0.999	S19	1.0
S10	0.994	S20	0.97
Average			0.9799

Table 4.7 shows the results of channels: C3, Cz, and C4 using the NN classifier. The table demostrates that S16 has the lowest true positive while S9 has the highest true positive. The overall average accuracy was 94.87%. While S16 got the lowest true positives, and one of the lowest false positive percentage of all the data.

The results can be seen in the ROC curve in Fig 4.4, where S16 is close to the half line, while the rest of the subject are way above the line. The areas on Table 4.8 show that subject S19 has the highest area under the ROC curve than all the other subjects, while S16 had the lowest ROC curve of all subjects. The average Area for the NN classifier was 0.97305. Comparing the averages of Table 4.6 with Table 4.8 the SVM classifier is a better classifier, than NN classifier.

Table 4.7: NN Confusion Matrix for Channels C3, C4, and Cz

		Outputs																			
		S1	S2	S3	S4	S5	S6	S7	S8	S9	S10	S11	S12	S13	S14	S15	S16	S17	S18	S19	S20	
Targets	S1	1268	0	0	0	0	0	16	1	0	0	0	3	0	2	8	0	0	20	0	2	96.06%
	S2	0	1305	0	0	0	2	0	0	0	1	0	9	0	0	3	0	0	0	0	0	98.86%
	S3	0	0	1315	0	0	0	0	0	0	0	0	0	2	0	0	1	0	0	0	2	99.62%
	S4	0	0	0	1314	0	0	0	0	0	0	0	0	0	0	0	0	0	6	0	0	99.55%
	S5	0	0	0	0	1295	10	0	1	10	0	0	3	0	0	0	0	1	0	0	0	98.11%
	S6	1	0	0	0	11	1182	0	17	0	0	10	67	0	0	18	0	9	4	0	1	89.55%
	S7	20	0	0	0	0	0	1291	3	0	0	0	0	0	0	0	0	0	6	0	0	97.8%
	S8	0	0	0	0	9	67	9	1123	0	0	19	13	2	0	23	6	9	14	11	15	85.08%
	S9	0	0	0	0	1	0	0	0	1303	0	0	0	0	0	0	0	0	0	16	0	98.71%
	S10	0	3	0	0	0	0	0	0	1	1303	0	7	0	0	4	0	2	0	0	0	98.71%
	S11	0	0	0	0	4	8	0	5	0	0	1291	2	0	0	0	0	0	0	0	10	97.8%
	S12	1	8	0	0	4	46	0	4	0	3	3	1128	0	0	103	0	13	3	0	4	85.45%
	S13	0	0	2	0	0	0	0	0	0	0	2	0	1311	0	0	5	0	0	0	0	99.32%
	S14	1	0	0	0	0	0	0	0	0	0	0	0	0	1319	0	0	0	0	0	0	99.92%
	S15	1	1	0	0	1	13	0	4	0	1	0	111	0	0	1187	0	0	1	0	0	89.92%
	S16	0	131	13	0	15	0	40	27	0	0	28	0	27	0	0	1035	0	0	0	4	78.41%
	S17	0	0	0	0	0	21	1	0	0	5	0	2	0	0	1	0	1290	0	0	0	97.73%
	S18	46	0	0	4	0	12	3	14	0	0	0	8	0	0	3	0	1	1226	0	3	92.88%
	S19	0	0	0	0	0	0	0	0	10	0	0	0	0	0	0	0	0	0	1310	0	99.24%
	S20	0	1	1	0	0	5	0	10	0	0	20	4	3	0	5	1	1	14	6	1249	94.62%
		88.62%	84.3%	91.95%	92.69%	89.96%	81.54%	88.58%	86.28%	91.5%	92.25%	87.81%	78.3%	90.76%	92.82%	82.15%	90.16%	90.57%	88.26%	90.82%	89.9%	94.87%

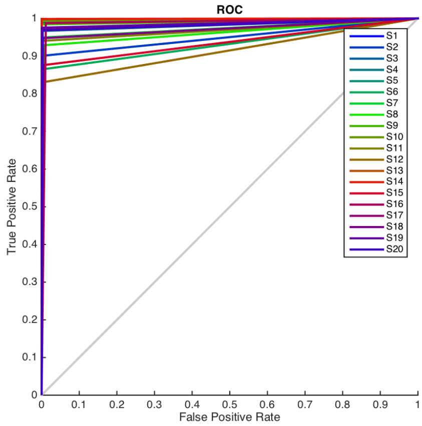

Fig 4.4: ROC figure for NN for channels C3, C4, and Cz

Table 4.8: ROC Area Under Curve for NN for Channels C3, Cz, and C4

Subject	Area	Subject	Area
S1	0.979	S11	0.987
S2	0.991	S12	0.923
S3	0.998	S13	0.996
S4	0.998	S14	1.0
S5	0.99	S15	0.946
S6	0.944	S16	0.892
S7	0.988	S17	0.988
S8	0.924	S18	0.963
S9	0.993	S19	0.996
S10	0.993	S20	0.972
Average			0.97305

4.3 Channels F3, Fz, F4

The confusion matrix on Table 4.9 shows S13 and S19 have the highest overall accuracy, while the lowest accuracy is for S1. The table shows that the average accuracy using the channels F3, Fz and F4 for all the partitions was 95.15%. While S1 has the lowest accuracy it also has the highest false positive rate than the other subjects. Many of S14 data got classified as S1 which increased S1 false positive percentage.

The ROC curve in Figure 4.5 shows that most of the data have similar true positive rates. The areas in Table 4.10 shows that the highest area of the ROC curves for each subject was S13 and S16. The lowest area was off subject S1. The average for all the areas was 0.9744

S5 and S13 have the highest overall accuracy for the NN classifier with a 99.85% accuracy shown in Table 4.11. The lowest accuracy shown in Table 4.11 is 70.38% for subject S10. The overall accuracy in the confusion matrix is 94.18%. Many of the data of S10 got misclassified as S2, which decreased the overall accuracy to 82.99%. While S10 has the lowest overall accuracy it isn't the subject with the highest false positive rate, which is S1, with only a 78.32% of true positives. The table shows us that many of S16 are classified as S3 which decreases the true positive. The ROC curve shown in Figure 4.6 illustrates the data for the classifier NN, S10 is the lowest one. The areas in Table 4.12 shows that the highest area of the ROC curves for each subject was of S13 and S5. The lowest area was off subject S10. The average for all the areas was 0.96945.

Comparing the results from Table 4.9 and Table 4.11, the results for S13 didn't change while the one for S16 did. While the lowest percentage that the SVM classier got was 85.0% the lowest that the NN classier got was 70.38%. The SVM classifer also got a better Overall average than the NN classifier. Comparing the averages of Table 4.10 with Table 4.12, it is shown that the SVM classifier classified better the data for the group of channels considered.

Table 4.9: SVM Confusion Matrix for Channels F3, Fz, and F4

Outputs

		S1	S2	S3	S4	S5	S6	S7	S8	S9	S10	S11	S12	S13	S14	S15	S16	S17	S18	S19	S20	
Targets	S1	1122	3	0	0	0	3	0	5	0	10	19	0	0	109	0	0	2	46	0	1	85.0%
	S2	4	1193	0	0	0	1	0	0	0	96	0	15	0	0	0	0	5	6	0	0	90.38%
	S3	0	0	1318	0	0	0	1	1	0	0	0	0	0	0	0	0	0	0	0	0	99.85%
	S4	0	0	0	1319	0	0	0	0	0	0	0	0	0	1	0	0	0	0	0	0	99.92%
	S5	0	0	0	0	1316	0	0	0	0	0	0	0	4	0	0	0	0	0	0	0	99.7%
	S6	1	17	0	0	0	1218	0	0	0	2	10	71	0	0	0	0	0	0	1	0	92.27%
	S7	0	0	0	0	0	0	1320	0	0	0	0	0	0	0	0	0	0	0	0	0	100.0%
	S8	5	0	0	0	0	0	0	1300	0	0	14	0	0	1	0	0	0	0	0	0	98.48%
	S9	0	0	0	0	0	1	0	0	1318	0	0	0	0	0	0	0	0	0	1	0	99.85%
	S10	7	112	0	0	0	9	0	0	0	1166	0	12	0	0	0	0	10	4	0	0	88.33%
	S11	22	0	0	0	0	6	0	23	0	0	1261	0	0	0	0	0	0	4	0	4	95.53%
	S12	0	23	0	0	0	78	0	0	0	11	0	1208	0	0	0	0	0	0	0	0	91.52%
	S13	0	0	0	0	0	0	0	0	0	0	0	0	1320	0	0	0	0	0	0	0	100.0%
	S14	135	0	0	0	0	0	0	1	0	1	0	0	0	1146	0	0	2	35	0	0	86.82%
	S15	0	1	0	0	0	3	0	0	0	0	0	6	0	0	1310	0	0	0	0	0	99.24%
	S16	0	0	0	0	7	0	0	0	0	0	0	0	4	0	0	1309	0	0	0	0	99.17%
	S17	15	21	0	0	0	0	0	0	0	35	0	2	0	4	0	0	1216	27	0	0	92.12%
	S18	56	4	3	1	0	2	0	0	0	11	17	0	0	38	0	0	19	1169	0	0	88.56%
	S19	0	0	0	0	0	0	0	0	0	0	0	0	0	0	0	0	0	0	1320	0	100.0%
	S20	0	1	0	0	0	7	0	0	0	0	38	2	0	0	0	0	0	1	0	1271	96.29%
		82.08%	86.76%	99.77%	99.92%	99.47%	91.72%	99.92%	97.74%	100.0%	87.54%	92.79%	91.79%	99.4%	88.22%	100.0%	100.0%	96.97%	90.48%	99.85%	99.61%	95.15%

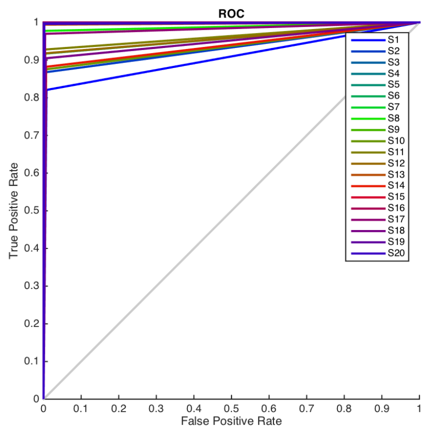

Fig 4.5: ROC figure for SVM for Channels F3, Fz, and F4

Table 4.10: ROC Area Under Curve for SVM for Channels F3, Fz, and F4

Subject	Area	Subject	Area
S1	0.92	S11	0.976
S2	0.948	S12	0.955
S3	0.999	S13	1.0
S4	1.0	S14	0.931
S5	0.998	S15	0.996
S6	0.959	S16	0.996
S7	1.0	S17	0.96
S8	0.992	S18	0.94
S9	0.999	S19	1.0
S10	0.938	S20	0.981
Average			0.9744

Table 4.11: NN Confusion Matrixr for channels F3, Fz, and F4

		Outputs																				
		S1	S2	S3	S4	S5	S6	S7	S8	S9	S10	S11	S12	S13	S14	S15	S16	S17	S18	S19	S20	
Targets	S1	1142	2	0	2	0	4	0	1	0	9	21	1	0	93	0	0	7	37	0	1	86.52%
	S2	4	1223	0	0	0	6	0	1	0	57	0	10	0	0	0	0	8	11	0	0	92.65%
	S3	0	0	1314	0	0	0	0	0	0	0	1	0	0	2	0	0	0	3	0	0	99.55%
	S4	0	0	0	1316	0	0	0	3	0	0	0	0	0	1	0	0	0	0	0	0	99.7%
	S5	0	0	0	0	1318	0	0	0	0	0	0	0	2	0	0	0	0	0	0	0	99.85%
	S6	5	10	0	0	0	1232	3	0	4	7	6	47	0	0	1	0	0	4	1	0	93.33%
	S7	0	0	3	0	3	0	1298	0	0	0	0	0	0	0	0	14	0	0	0	2	98.33%
	S8	2	0	0	4	1	0	0	1287	0	0	21	0	0	1	0	0	2	1	0	1	97.5%
	S9	0	1	0	0	0	2	0	0	1317	0	0	0	0	0	0	0	0	0	0	0	99.77%
	S10	8	108	2	0	0	27	82	30	1	929	38	29	0	11	1	0	25	19	10	0	70.38%
	S11	15	1	0	0	0	10	0	12	0	1	1257	1	0	0	0	0	0	12	0	11	95.23%
	S12	47	14	0	0	0	60	7	0	15	25	2	1101	0	0	28	0	9	11	0	1	83.41%
	S13	0	0	0	0	0	0	0	0	0	0	0	0	1318	0	0	1	0	0	0	1	99.85%
	S14	111	4	1	1	0	0	1	0	0	2	1	0	0	1158	0	0	3	38	0	0	87.73%
	S15	0	0	0	0	0	0	0	0	0	0	0	14	0	0	1305	0	1	0	0	0	98.86%
	S16	0	0	14	0	0	0	0	0	0	0	0	0	2	0	0	1304	0	0	0	0	98.79%
	S17	13	17	0	0	0	0	1	0	0	15	0	2	0	3	1	0	1236	32	0	0	93.64%
	S18	29	6	1	0	0	3	0	0	0	4	9	2	0	36	0	0	12	1218	0	0	92.27%
	S19	0	0	1	0	0	0	0	0	2	0	0	4	0	0	0	0	1	0	1312	0	99.39%
	S20	0	1	0	0	0	3	7	3	0	0	27	0	0	0	0	0	0	0	0	1279	96.89%
		78.32%	82.99%	91.52%	92.49%	92.72%	85.63%	86.6%	89.7%	91.52%	81.74%	85.17%	84.51%	92.73%	83.12%	90.88%	91.9%	88.22%	82.49%	92.21%	91.64%	94.18%

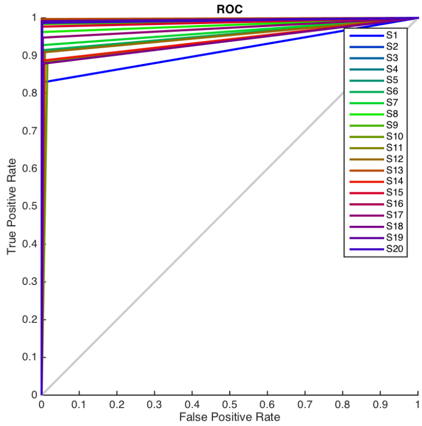

Fig 4.6: ROC figure for NN for channels F3, Fz, and F4

Table 4.12: ROC Area Under Curve for NN for Channels F3, Fz, and F4

Subject	Area	Subject	Area
S1	0.928	S11	0.974
S2	0.96	S12	0.915
S3	0.997	S13	0.999
S4	0.998	S14	0.936
S5	0.999	S15	0.994
S6	0.964	S16	0.994
S7	0.99	S17	0.967
S8	0.987	S18	0.958
S9	0.998	S19	0.997
S10	0.85	S20	0.984
Average			0.96945

4.4 Channels O1, O2, Pz

The overall accuracy for all subjects is 94.84% and it is shown in the confusion matrix in Table 4.13. The table shows that the subject with the highest accuracy for channels O1, O2, and Pz is S19 that has a 100% accuracy with all partitions, while S20 has a 20.80% which makes it the lowest accuracy. The confusion matrix also shows that many of the data of S20 got misclassified as S8 and S11, which increased false positive percentage. While S20 had the highest accuracy some of the data of S9 and S13 are misclassified as S20.

Figure 4.7 shows how the ROC curve for O1, O2 and Pz and the areas under curves are in Table 4.14. The highest area under the curve is off subject S19, while the lowest is of subject S20. The average off all the area was 96.6235%.

The highest accuracy in the confusion matrix in Table 4.15 is 99.55% for S19 , while the lowest is 29.92% for S16. The average accuracy for all the data classified with NN is 90.42%. The subject with the highest false positive is S8 that has 23.31% of false positive, most of those false positive, were misclassification from S16.

The ROC curve in Figure 4.8 shows the difference between S16 results and the rest of the subjects. The areas in Table 4.16 are of the ROC curves. The subject with the highest area was S15, while the lowest area was off subject S16 with the NN classifier. The average area was 87.13%.

Comparing the results from Table 4.13 and Table 4.11, S16 in the former has an accuracy of 99.32%, while in the later S16 had an accuracy of 29.92%. S14 in Table 4.13 has an accuracy of 79.62%, while on Table 4.13 S14 has an accuracy 85.38% The overall accuracy for SVM classifier was higher than that for NN classifier. Comparing the averages of the ROCs curves the SVM classifier is a better classifier using the Channels O1, O2, and Pz.

Table 4.13: SVM Confusion Matrix for Channels O1, O2, and Pz

		Outputs																				
		S1	S2	S3	S4	S5	S6	S7	S8	S9	S10	S11	S12	S13	S14	S15	S16	S17	S18	S19	S20	
Targets	S1	1270	0	0	0	0	0	0	8	0	0	12	0	0	6	0	0	6	0	0	18	96.21%
	S2	0	1314	0	0	0	3	0	1	0	0	1	0	0	0	0	0	0	0	0	1	99.55%
	S3	0	0	1317	0	0	0	0	0	0	2	0	0	1	0	0	0	0	0	0	0	99.77%
	S4	0	0	0	1302	0	0	0	0	0	3	0	0	14	0	0	0	0	1	0	0	98.64%
	S5	0	0	0	1	1313	0	0	0	0	0	0	0	6	0	0	0	0	0	0	0	99.47%
	S6	0	0	1	0	0	1318	0	0	0	1	0	0	0	0	0	0	0	0	0	0	99.85%
	S7	0	3	0	0	0	0	1317	0	0	0	0	0	0	0	0	0	0	0	0	0	99.77%
	S8	5	5	1	0	0	0	0	1172	0	0	52	6	0	14	0	0	3	0	0	62	88.79%
	S9	0	0	0	0	0	0	0	0	1319	0	0	0	0	0	0	0	0	1	0	0	99.92%
	S10	0	0	5	7	0	8	0	0	0	1293	0	0	7	0	0	0	0	0	0	0	97.95%
	S11	6	2	1	0	0	4	0	88	0	0	1125	18	7	16	0	0	1	0	0	52	85.23%
	S12	0	0	8	0	0	21	1	39	0	0	40	1147	1	35	0	0	23	0	0	5	86.89%
	S13	0	0	1	37	0	4	1	1	1	5	1	0	1263	2	0	0	1	0	0	3	95.68%
	S14	3	0	0	0	0	1	0	41	0	0	24	57	5	1133	0	0	38	0	0	18	85.83%
	S15	0	0	1	0	0	0	0	0	0	1	0	0	0	0	1318	0	0	0	0	0	99.85%
	S16	5	13	0	0	0	0	0	0	0	0	0	0	0	0	0	1302	0	0	0	0	98.64%
	S17	6	0	0	0	0	0	0	3	0	0	11	30	0	48	0	0	1220	0	0	2	92.42%
	S18	0	0	0	0	0	5	0	0	1	0	0	0	0	0	1	0	0	1313	0	0	99.47%
	S19	0	0	0	0	0	0	0	0	0	0	0	0	0	0	0	0	0	0	1320	0	100.0%
	S20	40	4	0	1	0	4	0	153	0	2	101	10	24	16	0	0	4	0	0	961	72.8%
		95.13%	97.99%	98.65%	96.59%	100.0%	96.35%	99.85%	77.82%	99.85%	98.93%	82.3%	90.46%	95.11%	89.21%	99.92%	100.0%	94.14%	99.85%	100.0%	85.65%	94.84%

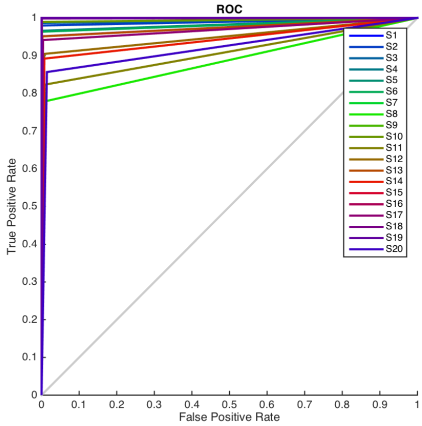

Fig 4.7: ROC figure for NN for channels O1, O2, and Pz

Table 4.14: ROC Area Under Curve for SVM for Channels O1, O2, and Pz

Subject	Area	Subject	Area
S1	0.98	S11	0.921
S2	0.997	S12	0.932
S3	0.999	S13	0.977
S4	0.992	S14	0.926
S5	0.997	S15	0.999
S6	0.998	S16	0.993
S7	0.999	S17	0.961
S8	0.937	S18	0.997
S9	1.0	S19	1.0
S10	0.989	S20	0.861
Average			0.97275

Table 4.15: SVM Confusion Matrix for Channels O1, O2, and Pz

	Outputs																				
Targets		S1	S2	S3	S4	S5	S6	S7	S8	S9	S10	S11	S12	S13	S14	S15	S16	S17	S18	S19	S20	
	S1	1255	1	0	0	0	0	0	9	0	0	15	0	0	8	0	2	5	0	0	25	95.08%
	S2	1	1303	0	0	0	3	0	2	0	0	0	0	0	0	0	1	0	0	0	10	98.71%
	S3	0	0	1310	0	0	0	0	0	0	3	0	1	0	0	6	0	0	0	0	0	99.24%
	S4	0	0	0	1303	0	0	0	0	0	5	0	0	10	1	0	0	0	0	0	1	98.71%
	S5	0	0	0	0	1313	0	0	0	0	0	0	0	4	3	0	0	0	0	0	0	99.47%
	S6	0	1	3	0	0	1290	0	0	0	5	1	3	0	0	0	0	0	11	3	3	97.73%
	S7	0	10	0	0	0	2	1276	9	0	0	3	0	0	0	0	0	0	16	0	4	96.67%
	S8	6	5	0	0	0	2	0	1149	0	0	53	13	1	20	0	0	10	0	0	61	87.05%
	S9	0	0	0	0	0	0	0	0	1319	0	0	0	0	0	0	0	0	0	1	0	99.92%
	S10	0	2	9	4	0	118	1	0	0	1156	0	7	16	0	5	0	0	1	0	1	87.58%
	S11	0	6	0	0	0	1	0	54	0	1	1162	25	5	14	0	0	3	0	0	49	88.03%
	S12	0	0	0	0	0	9	0	17	0	0	31	1192	6	31	0	0	30	0	0	4	90.3%
	S13	0	0	0	23	2	6	0	3	0	8	5	10	1241	6	0	0	3	0	0	13	94.02%
	S14	3	0	0	0	0	0	1	18	0	0	21	62	9	1163	0	0	29	0	0	14	88.11%
	S15	0	0	0	0	0	1	0	0	0	1	0	0	0	0	1318	0	0	0	0	0	99.85%
	S16	62	34	0	0	0	5	0	98	0	71	136	86	0	0	64	634	0	104	0	26	48.03%
	S17	2	0	0	0	0	0	0	1	0	0	6	14	0	52	0	0	1241	0	0	4	94.02%
	S18	0	0	0	0	0	3	0	0	1	0	0	0	0	0	0	0	0	1316	0	0	99.7%
	S19	0	0	0	0	0	0	0	0	0	0	0	0	1	0	0	0	0	0	1319	0	99.92%
	S20	24	6	0	2	0	8	0	95	0	3	97	30	20	17	0	0	5	0	0	1013	76.74%
		86.66%	88.88%	92.21%	91.21%	92.79%	83.53%	92.61%	74.96%	92.9%	85.51%	72.07%	77.73%	88.13%	82.82%	88.28%	86.02%	87.39%	85.02%	92.69%	77.11%	91.94%

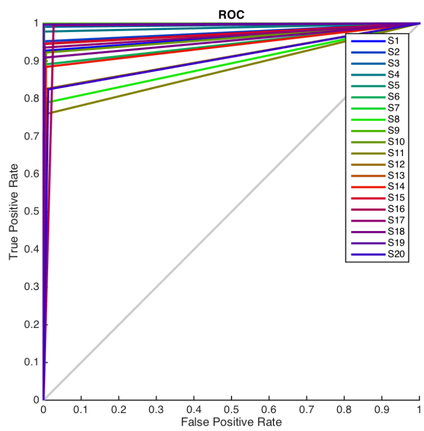

Fig 4.8: ROC figure for NN for channels O1, O2, and Pz

Table 4.16: ROC Area Under Curve for NN for Channels O1, O2, and Pz

Subject	Area	Subject	Area
S1	0.973	S11	0.933
S2	0.992	S12	0.947
S3	0.996	S13	0.969
S4	0.993	S14	0.938
S5	0.997	S15	0.998
S6	0.985	S16	0.74
S7	0.983	S17	0.968
S8	0.929	S18	0.996
S9	1.0	S19	1.0
S10	0.936	S20	0.879
Average			0.9576

4.5 Channels: C3, C4, FC5, FC6

The confusion matrix in Table 4.17 shows the results for channels C3, C4, FC5, and FC6 using the SVM classifier. Subjects S3, S7, S9, S11, and S19 have the highest accuracy with a percentage of 100.0% for all data, while subject S14 has the lowest accuracy with 88.70%. The table shows that the average accuracy of the SVM classifier using channels C3, C4, FC5, and FC6 is 98.02%. The confusion matrix also shows that the lowest percentage 89.33% belongs to S1, while subject S4, S16, and S19 have the highest true positive percentage with 100%.

The ROC curve displayed in Figure 4.9 shows how the data is close together, while the areas under those curves are shown in Table 4.18. The highest area under the curve was for subjects S3, S9, S19, while the lowest area belongs to subject S18. The average for the ROC cuves was for .98075.

The confusion matrix in Table 4.19 shows the result for the NN classifier with channels C3, C4, FC5, and FC6. The highest accuracy results for the classifier was for subject S19 with an accuracy of 99.92%, while the lowest is for subject S4 with an accuracy of 49.82% percent. The average accuracy for the NN classifier is 93.22%, while the lowest true positive percentage is for S1.

The ROC curve shown in Figure 4.10 shows how low S4 is compared to the rest of the data. Table 4.20 shows that the highest area for the ROC curve using NN classifier was S19 and the lowest area was for S4. The average area for the NN classifier was 0.96435.

The results of Table 4.17 compared with Table 4.19 show that S4 has a higher accuracy with the SVM classifier than with the NN classifier. It also shows that subject S14 does better with the NN classifier where it gets a 95.08% and with SVM classifier it gets 89.17%. Comparing the confusion matrices also shows that the SVM classifier has an average accuracy of 96.34%, while the NN classifier has 93.22% accuracy. Comparing the SVM classifier ROC curves with the NN classifier ROC curves, it is shown that the SVM classifier is better.

Table 4.17: SVM Confusion Matrix for channels C3, C4, FC5, and FC6

		Outputs																				
		S1	S2	S3	S4	S5	S6	S7	S8	S9	S10	S11	S12	S13	S14	S15	S16	S17	S18	S19	S20	
Targets	S1	1184	0	0	0	0	14	0	0	0	3	0	0	1	54	0	0	0	64	0	0	89.7%
	S2	0	1286	0	0	0	4	0	0	0	5	0	24	0	0	0	0	0	1	0	0	97.42%
	S3	0	0	1320	0	0	0	0	0	0	0	0	0	0	0	0	0	0	0	0	0	100.0%
	S4	0	0	0	1318	0	0	0	0	0	0	0	0	0	0	0	0	0	2	0	0	99.85%
	S5	0	0	0	0	1309	4	0	0	5	0	0	0	0	0	0	1	1	0	0	0	99.17%
	S6	1	4	2	0	3	1280	0	21	0	1	1	1	4	0	0	0	0	1	0	1	96.97%
	S7	1	0	0	0	0	0	1319	0	0	0	0	0	0	0	0	0	0	0	0	0	99.92%
	S8	5	0	0	0	0	30	1	1262	0	1	0	1	17	0	0	0	0	3	0	0	95.61%
	S9	0	0	0	0	0	0	0	0	1320	0	0	0	0	0	0	0	0	0	0	0	100.0%
	S10	10	21	0	0	0	1	0	9	0	1215	2	50	0	0	3	0	3	4	0	2	92.05%
	S11	0	0	0	0	0	0	0	0	0	1	1316	0	0	0	0	1	0	0	0	2	99.7%
	S12	0	14	0	0	0	29	0	8	0	35	3	1207	3	1	4	2	0	10	0	4	91.44%
	S13	2	0	0	0	0	14	3	26	0	1	0	3	1258	0	0	0	0	1	0	12	95.3%
	S14	87	0	0	1	0	0	0	0	0	6	0	0	0	1224	1	0	0	1	0	0	92.73%
	S15	0	3	0	0	0	0	0	0	0	0	4	4	0	0	1309	0	0	0	0	0	99.17%
	S16	0	0	0	0	1	0	0	0	20	1	9	2	0	0	0	1287	0	0	0	0	97.5%
	S17	0	0	0	0	0	0	0	0	0	3	0	0	0	0	0	0	1316	0	0	1	99.7%
	S18	66	3	0	3	0	1	0	17	0	24	0	19	6	2	0	0	2	1177	0	0	89.17%
	S19	0	0	0	0	0	0	0	0	0	0	0	0	0	0	0	0	0	0	1320	0	100.0%
	S20	0	0	0	0	0	11	1	28	0	15	6	6	37	0	0	0	4	5	0	1207	91.44%
		87.32%	96.62%	99.85%	99.7%	99.7%	92.22%	99.62%	92.05%	98.14%	92.68%	98.14%	91.65%	94.87%	95.55%	99.39%	99.69%	99.25%	92.75%	100.0%	98.21%	96.34%

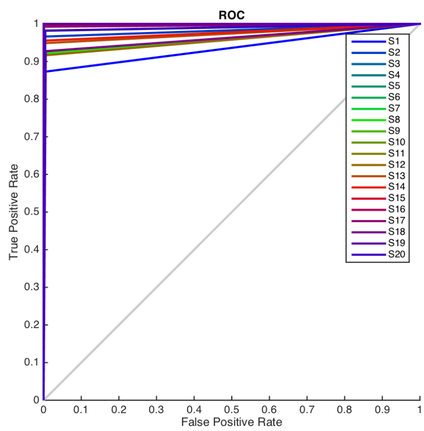

Fig 4.9: ROC figure for SVM for channels C3, C4, FC5, and FC6

Table 4.18: ROC Area Under Curve for SVM for Channels: C3, C4, FC5 and FC6

Subject	Area	Subject	Area
S1	0.945	S11	0.998
S2	0.986	S12	0.955
S3	1.0	S13	0.975
S4	0.999	S14	0.962
S5	0.996	S15	0.996
S6	0.983	S16	0.987
S7	1.0	S17	0.998
S8	0.976	S18	0.944
S9	1.0	S19	1.0
S10	0.958	S20	0.957
Average			0.98075

Table 4.19: NN Confusion Matrix for Channels C3, C4, FC5, and FC6

		Outputs																				
		S1	S2	S3	S4	S5	S6	S7	S8	S9	S10	S11	S12	S13	S14	S15	S16	S17	S18	S19	S20	
Targets	S1	1202	0	0	2	0	6	3	3	0	4	0	3	6	50	0	0	0	39	0	2	91.06%
	S2	0	1294	0	0	0	1	0	0	0	2	1	15	0	2	0	0	0	4	0	1	98.03%
	S3	0	0	1313	0	2	0	0	0	0	0	0	0	0	0	0	1	2	0	0	2	99.47%
	S4	144	0	0	659	0	0	118	95	0	45	0	0	0	153	0	0	5	88	0	13	49.92%
	S5	0	0	3	0	1172	6	4	1	1	8	0	13	0	3	0	6	5	0	1	97	88.79%
	S6	2	0	8	0	6	1266	0	11	0	1	0	11	4	2	0	0	0	1	0	8	95.91%
	S7	0	0	0	0	0	0	1316	2	0	0	0	0	0	1	0	0	0	0	0	1	99.7%
	S8	4	3	0	0	0	14	6	1234	1	5	0	3	36	1	0	0	0	7	0	6	93.48%
	S9	0	0	0	0	0	1	0	0	1312	0	1	0	2	0	0	3	0	0	1	0	99.39%
	S10	9	8	1	0	1	2	0	8	0	1177	5	48	5	6	11	2	20	10	0	7	89.17%
	S11	0	1	0	0	0	0	0	0	2	3	1302	2	3	0	0	7	0	0	0	0	98.64%
	S12	0	14	1	0	0	10	0	4	0	39	3	1213	4	0	16	3	0	5	0	8	91.89%
	S13	3	0	1	0	0	7	0	30	1	0	0	3	1265	0	1	0	0	2	0	7	95.83%
	S14	49	4	0	0	0	0	0	0	0	0	0	3	0	1255	2	0	0	7	0	0	95.08%
	S15	0	5	0	0	0	0	0	0	0	6	2	5	0	0	1300	1	0	1	0	0	98.48%
	S16	0	0	1	0	1	0	0	0	1	0	32	0	0	0	0	1285	0	0	0	0	97.35%
	S17	3	0	0	0	2	0	0	0	0	10	0	0	0	1	0	2	1298	0	0	4	98.33%
	S18	34	2	0	1	0	2	0	12	0	6	0	11	0	5	0	2	0	1245	0	0	94.32%
	S19	0	0	0	0	0	0	0	0	1	0	0	0	0	0	0	0	0	0	1319	0	99.92%
	S20	2	2	0	0	1	8	1	14	1	19	6	17	58	0	0	0	4	4	0	1183	89.62%
		78.09%	90.51%	91.96%	86.52%	91.23%	89.46%	85.03%	81.94%	92.52%	83.02%	89.78%	84.32%	85.6%	79.71%	90.95%	91.03%	90.56%	82.68%	92.82%	82.31%	93.22%

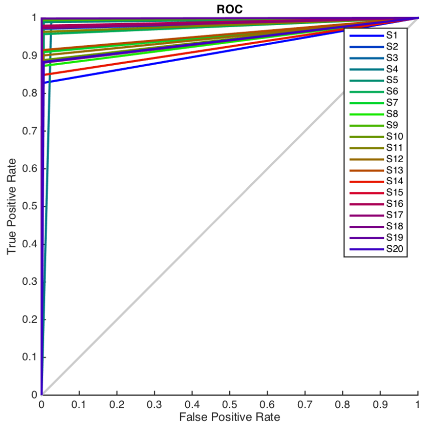

Fig 4.10: ROC figure for NN for channels C3, C4, FC5, and FC6

Table 4.20: ROC Area Under Curve for NN for Channels: C3, C4, FC5 and FC6

Subject	Area	Subject	Area
S1	0.95	S11	0.992
S2	0.989	S12	0.957
S3	0.997	S13	0.977
S4	0.75	S14	0.971
S5	0.944	S15	0.992
S6	0.978	S16	0.986
S7	0.996	S17	0.991
S8	0.964	S18	0.968
S9	0.997	S19	1.0
S10	0.943	S20	0.945
Average			0.96435

4.6 Channels:C3, C4, FC1, FC2, FC5, FC6

The confusion matrix on Table 4.21 shows the results for channels C3, C4, FC1, FC2, FC5, and FC6 using the SVM classifier. The subjects with the highest accuracys are S11, S16, and S19, while the subject with the lowest accuracy is for S14. The average accuracy for the SVM classifier with channels C3, C4, FC1, FC2, FC5, and FC6 is 97.76%, it also shows that the lowest true positive percentage was for subject S1 with 88.24%.

The ROC curve for the SVM classifier is shown in Figure 4.11 and the area under the ROC curve is shown in Table 4.22. The highest area under the curve was from subject

S3, S7, S9, S11, and S19, while the lowest was from S14. The average for all the ROC curves with the SVM classifier was 0.9896

Table 4.21: SVM Confusion Matrix for Channels C3, C4, FC1, FC2, FC5, and FC6

		Outputs																				
		S1	S2	S3	S4	S5	S6	S7	S8	S9	S10	S11	S12	S13	S14	S15	S16	S17	S18	S19	S20	
Targets	S1	1180	0	0	0	0	9	0	0	0	0	0	1	1	122	0	0	1	6	0	0	89.39%
	S2	0	1317	0	0	0	1	0	0	0	0	0	0	0	0	2	0	0	0	0	0	99.77%
	S3	0	0	1320	0	0	0	0	0	0	0	0	0	0	0	0	0	0	0	0	0	100.0%
	S4	2	0	0	1317	0	0	0	0	0	0	0	0	0	0	0	0	0	1	0	0	99.77%
	S5	0	0	0	0	1306	5	0	0	1	0	0	0	0	0	0	0	8	0	0	0	98.94%
	S6	0	2	0	0	2	1309	0	2	2	1	0	2	0	0	0	0	0	0	0	0	99.17%
	S7	0	0	0	0	0	0	1320	0	0	0	0	0	0	0	0	0	0	0	0	0	100.0%
	S8	0	0	0	0	0	4	0	1306	0	0	0	0	6	0	0	0	0	4	0	0	98.94%
	S9	0	0	0	0	0	0	0	0	1320	0	0	0	0	0	0	0	0	0	0	0	100.0%
	S10	0	11	0	0	0	0	0	0	0	1309	0	0	0	0	0	0	0	0	0	0	99.17%
	S11	0	0	0	0	0	0	0	0	0	0	1320	0	0	0	0	0	0	0	0	0	100.0%
	S12	0	0	0	0	2	14	0	11	5	0	0	1268	6	6	7	0	0	1	0	0	96.06%
	S13	0	0	0	0	0	13	2	13	6	1	0	3	1282	0	0	0	0	0	0	0	97.12%
	S14	128	2	0	0	0	0	0	1	0	1	0	13	0	1172	0	0	0	3	0	0	88.79%
	S15	0	15	0	0	0	0	0	0	0	6	4	4	0	0	1291	0	0	0	0	0	97.8%
	S16	0	0	6	0	0	0	0	0	4	0	0	0	0	0	0	1310	0	0	0	0	99.24%
	S17	0	0	0	0	11	0	0	0	0	0	0	0	0	0	0	0	1309	0	0	0	99.17%
	S18	11	0	0	0	0	1	0	5	0	0	0	6	1	2	0	0	0	1294	0	0	98.03%
	S19	0	0	0	0	0	0	0	0	0	0	0	0	0	0	0	0	0	0	1320	0	100.0%
	S20	0	0	4	0	0	0	0	9	0	0	0	0	0	0	0	0	0	0	0	1307	99.02%
		89.33%	97.77%	99.25%	100.0%	98.86%	96.53%	99.85%	96.96%	98.65%	99.32%	99.7%	97.76%	98.92%	90.02%	99.31%	100.0%	99.32%	98.85%	100.0%	100.0%	98.02%

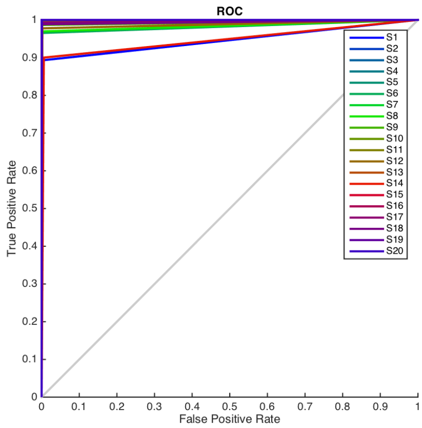

Fig 4.11: ROC figure for NN for channels C3, C4, FC1, FC2, FC5, and FC6

Table 4.22: ROC Area Under Curve for SVM for channels C3, C4, FC1, FC2, FC5 and FC6

Subject	Area	Subject	Area
S1	0.944	S11	1.0
S2	0.998	S12	0.98
S3	1.0	S13	0.985
S4	0.999	S14	0.941
S5	0.994	S15	0.989
S6	0.995	S16	0.996
S7	1.0	S17	0.996
S8	0.994	S18	0.99
S9	1.0	S19	1.0
S10	0.996	S20	0.995
Average			0.9896

The confusion matrix in Table 4.23 shows the average for the NN classifier and the subjects with the highest accuracy were S4, S7, and S19 with 100%, while the subject with the lowest accuracy is S18 with 86.59 %. The confusion matrix shows that the average accuracy is 9726%, while the lowest true positive percentage is S14.

The ROC curve for the NN classifier accuracy is on Figure 4.12, and the area of those curves are displayed in Table 4.24. The highest area on the table is from subject S4, while the lowest area was from subject S1. The average area for NN classifier was 0.98565.

The results of Table 4.21 compared with Table 4.23 show that S4 has a higher accuracy with the NN classifier than with the SVM classifier, while S16 has a higher accuracy with the SVM classifier than with the NN classifier. Comparing the confusion matrix in Table 4.21 with the confusion matrix in Table 4.23, the SVM classifier has an average accuracy of 98.02%, while the NN classifier has a 97.26% accuracy, which makes the NN classifier good for the channels: C3, C4, FC1, FC2, FC5 and FC6. Based on the averages of the areas under the ROC curve tables the SVM classifier did better compared with the NN classifier.

Table 4.23: NN Confusion Matrix for Channels C3, C4, FC1, FC2, FC5, and FC6

		Outputs																				
		S1	S2	S3	S4	S5	S6	S7	S8	S9	S10	S11	S12	S13	S14	S15	S16	S17	S18	S19	S20	
Targets	S1	1175	0	0	0	0	7	1	0	0	0	0	1	8	122	0	0	2	4	0	0	89.02%
	S2	3	1303	0	0	0	1	0	0	1	3	1	2	0	0	5	0	1	0	0	0	98.71%
	S3	0	0	1312	0	0	0	0	0	0	2	0	0	0	0	6	0	0	0	0	0	99.39%
	S4	0	0	0	1320	0	0	0	0	0	0	0	0	0	0	0	0	0	0	0	0	100.0%
	S5	0	0	0	0	1302	2	0	1	2	0	0	2	0	0	0	0	11	0	0	0	98.64%
	S6	5	2	0	0	4	1295	0	4	1	3	1	0	5	0	0	0	0	0	0	0	98.11%
	S7	0	0	0	0	0	0	1320	0	0	0	0	0	0	0	0	0	0	0	0	0	100.0%
	S8	0	0	0	0	0	2	2	1299	0	0	1	3	10	0	0	0	0	3	0	0	98.41%
	S9	0	0	0	0	0	1	0	0	1303	0	0	0	8	0	0	0	0	0	8	0	98.71%
	S10	1	8	0	0	2	2	0	0	1	1304	0	0	2	0	0	0	0	0	0	0	98.79%
	S11	0	0	0	0	0	0	0	1	0	0	1317	0	0	0	1	0	1	0	0	0	99.77%
	S12	0	0	0	0	2	5	0	5	7	1	7	1275	7	6	3	0	1	1	0	0	96.59%
	S13	2	2	0	0	0	7	0	10	2	5	0	19	1270	0	0	0	0	3	0	0	96.21%
	S14	88	2	0	0	0	0	0	0	0	2	0	13	1	1212	0	0	0	2	0	0	91.82%
	S15	0	9	0	0	0	0	0	0	0	2	0	4	0	0	1305	0	0	0	0	0	98.86%
	S16	0	2	23	0	0	0	0	0	0	0	0	0	0	0	0	1295	0	0	0	0	98.11%
	S17	1	0	0	0	3	1	0	0	0	0	0	0	0	0	0	0	1315	0	0	0	99.62%
	S18	20	0	0	12	0	0	46	24	0	0	0	52	0	15	2	0	0	1143	0	6	86.59%
	S19	0	0	0	0	0	0	0	0	0	0	0	0	0	0	0	0	0	0	1320	0	100.0%
	S20	0	3	0	0	0	0	0	7	0	0	0	3	7	0	0	2	0	6	0	1292	97.88%
		84.88%	91.2%	91.48%	92.18%	92.22%	91.23%	89.87%	89.71%	92.04%	91.75%	92.31%	86.63%	89.63%	83.87%	91.82%	92.7%	91.94%	90.65%	92.44%	92.42%	97.26%

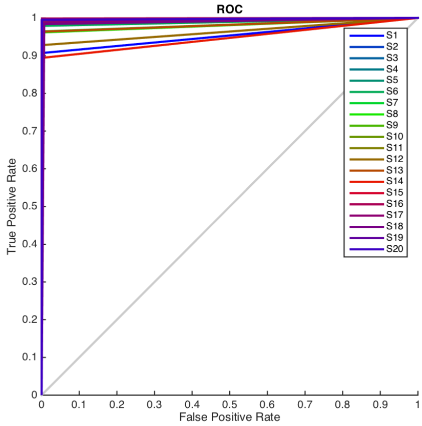

Fig 4.12: ROC figure for NN for channels C3, C4, FC1, FC2, FC5, and FC6

Table 4.24: ROC Area Under Curve for NN for channels C3, C4, FC1, FC2, FC5 and FC6

Subject	Area	Subject	Area
S1	0.943	S11	0.999
S2	0.993	S12	0.981
S3	0.997	S13	0.98
S4	1.0	S14	0.956
S5	0.993	S15	0.994
S6	0.99	S16	0.99
S7	0.999	S17	0.998
S8	0.991	S18	0.933
S9	0.993	S19	1.0
S10	0.994	S20	0.989
Average			0.98565

4.7 Channels:C3, C4, F3, F4, FC1, FC2, FC5, FC6

The confusion matrix in Table 4.25 shows that the subjects with the highest accuracy for the SVM classifier were S4, S7, and S19 with and accuracy 100%, while the lowest accuracy is for subject S18 with 86.56%. The confusion matrix shows that the average accuracy was 97.26%.

The ROC curve for the SVM classifier accuracy is shown in Figure 4.13, with the area under the ROC curve shown in Table 4.26. The subjects with the highest area were S4, S7, S17, and S19, while the lowest S1. The average area on the table was .0.9852.

The confusion matrix in Table 4.27 shows that the subjects with the highest accuracy for the NN classifier was S19 with an accuracy of 100.00% while the lowest accuracy is of subject S1 with 82.95%. The confusion matrix shows that the average accuracy was 96.76%.

The ROC curve for the SVM classifier accuracy is in Figure 4.14, with the area under the ROC curve in Table 4.28. The subject with the highest area was S19, while the lowest was for S14. The average area in the table is 0.98295.

Comparing the results of Table 4.25 with Table 4.27 it is shown that in the former table, 3 subjects had an accuracy of 100.0%, while 1 of the subjects using the NN classifier had a 100.00%. The SVM classifier had better results overall with an average accuracy is 97.18%, while NN classifier average accuracy is 96.76%. Comparing the results for the area, SVM was a better classifier for this group of channels than NN.

Table 4.25: SVM results for channels C3, C4, F3, F4, FC1, FC2, FC5, and FC6

		Outputs																				
		S1	S2	S3	S4	S5	S6	S7	S8	S9	S10	S11	S12	S13	S14	S15	S16	S17	S18	S19	S20	
Targets	S1	1088	0	0	0	0	18	1	0	0	0	0	13	10	187	0	0	0	3	0	0	82.42%
	S2	1	1313	0	0	0	0	0	0	0	6	0	0	0	0	0	0	0	0	0	0	99.47%
	S3	0	0	1318	0	0	0	0	0	2	0	0	0	0	0	0	0	0	0	0	0	99.85%
	S4	0	0	0	1320	0	0	0	0	0	0	0	0	0	0	0	0	0	0	0	0	100.0%
	S5	0	0	0	0	1314	0	0	0	3	0	0	0	0	0	0	0	2	0	1	0	99.55%
	S6	12	0	0	0	0	1293	0	0	2	0	1	9	3	0	0	0	0	0	0	0	97.95%
	S7	0	0	0	0	0	0	1320	0	0	0	0	0	0	0	0	0	0	0	0	0	100.0%
	S8	0	0	0	0	0	0	0	1314	0	0	0	0	0	0	0	0	0	6	0	0	99.55%
	S9	0	0	0	0	0	1	0	0	1314	0	0	0	5	0	0	0	0	0	0	0	99.55%
	S10	0	4	0	0	1	0	0	0	1	1313	0	0	0	0	1	0	0	0	0	0	99.47%
	S11	0	0	0	0	2	0	0	0	2	0	1316	0	0	0	0	0	0	0	0	0	99.7%
	S12	11	0	0	0	0	18	0	2	2	1	1	1261	1	7	9	0	0	7	0	0	95.53%
	S13	1	0	1	0	0	9	1	1	26	0	1	4	1276	0	0	0	0	0	0	0	96.67%
	S14	184	1	0	0	0	1	0	3	0	1	0	20	0	1107	0	0	0	3	0	0	83.86%
	S15	0	5	0	0	0	2	0	0	0	5	12	20	0	0	1276	0	0	0	0	0	96.67%
	S16	0	0	23	0	0	0	0	0	0	0	0	0	0	0	0	1296	0	0	1	0	98.18%
	S17	0	0	0	0	1	0	0	0	0	0	0	0	0	0	0	0	1319	0	0	0	99.92%
	S18	13	0	0	0	0	1	0	10	0	0	0	6	0	4	0	0	0	1286	0	0	97.42%
	S19	0	0	0	0	0	0	0	0	0	0	0	0	0	0	0	0	0	0	1320	0	100.0%
	S20	0	0	2	0	0	4	0	0	0	0	0	12	11	0	0	0	0	0	0	1291	97.8%
		83.05%	99.24%	98.07%	100.0%	99.7%	95.99%	99.85%	98.8%	97.19%	99.02%	98.87%	93.75%	97.7%	84.83%	99.22%	100.0%	99.85%	98.54%	99.85%	100.0%	97.18%

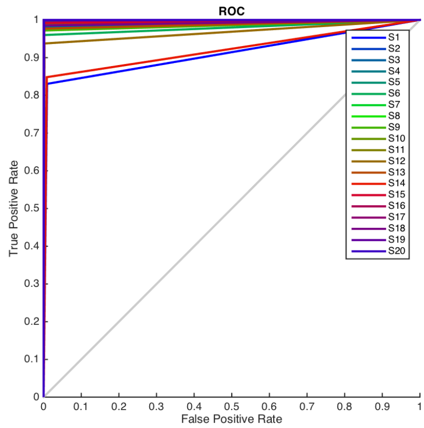

Fig 4.13: ROC figure for NN for channel C3, C4, F3, F4, FC1, FC2, FC5, and FC6

Table 4.26: ROC Area Under Curve for SVM for Channels:C3, C4, F3, F4, FC1, FC2, FC5, and FC6

Subject	Area	Subject	Area
S1	0.908	S11	0.998
S2	0.997	S12	0.976
S3	0.999	S13	0.983
S4	1.0	S14	0.915
S5	0.998	S15	0.983
S6	0.989	S16	0.991
S7	1.0	S17	1.0
S8	0.997	S18	0.987
S9	0.997	S19	1.0
S10	0.997	S20	0.989
Average			0.9852

Table 4.27: NN Confusion Matrix for Channels C3, C4, F3, F4, FC1, FC2, FC5, and FC6

		Outputs																				
		S1	S2	S3	S4	S5	S6	S7	S8	S9	S10	S11	S12	S13	S14	S15	S16	S17	S18	S19	S20	
Targets	S1	1095	0	0	0	0	19	0	0	0	0	0	20	10	169	1	0	0	6	0	0	82.95%
	S2	2	1310	0	0	0	0	0	0	0	3	0	0	0	1	3	0	1	0	0	0	99.24%
	S3	0	0	1318	0	0	0	0	0	0	1	0	0	0	0	0	1	0	0	0	0	99.85%
	S4	0	0	0	1320	0	0	0	0	0	0	0	0	0	0	0	0	0	0	0	0	100.0%
	S5	0	0	0	0	1304	2	0	3	1	2	2	0	0	0	0	0	6	0	0	0	98.79%
	S6	21	0	0	0	0	1292	0	0	2	0	0	4	1	0	0	0	0	0	0	0	97.88%
	S7	0	0	0	0	0	0	1318	0	0	1	0	0	1	0	0	0	0	0	0	0	99.85%
	S8	0	2	0	0	1	0	0	1302	0	0	1	3	0	2	0	0	0	9	0	0	98.64%
	S9	0	0	0	0	0	0	0	0	1304	1	0	0	13	0	0	0	0	0	2	0	98.79%
	S10	1	3	0	0	2	0	0	0	1	1296	0	1	0	12	4	0	0	0	0	0	98.18%
	S11	0	0	0	0	0	0	0	3	8	0	1298	11	0	0	0	0	0	0	0	0	98.33%
	S12	5	0	0	0	1	12	0	5	1	3	6	1257	5	9	8	0	0	8	0	0	95.23%
	S13	1	0	0	0	0	2	1	0	13	0	0	2	1295	0	0	0	0	0	6	0	98.11%
	S14	136	1	0	1	0	0	0	0	0	1	0	20	0	1153	4	0	0	4	0	0	87.35%
	S15	0	1	0	0	0	2	0	0	0	0	13	9	0	1	1294	0	0	0	0	0	98.03%
	S16	0	8	21	38	0	0	0	2	0	0	0	0	3	41	10	1176	0	16	0	5	89.09%
	S17	0	0	0	0	1	0	0	0	0	3	0	0	0	0	0	0	1316	0	0	0	99.7%
	S18	5	0	0	0	4	0	0	5	0	0	0	14	0	10	0	0	0	1282	0	0	97.12%
	S19	0	0	0	0	0	0	0	0	0	0	0	0	0	0	0	0	0	0	1320	0	100.0%
	S20	0	0	0	0	0	0	0	0	0	0	0	15	6	0	0	5	0	0	0	1294	98.03%
		81.17%	91.98%	91.71%	90.47%	92.31%	90.67%	92.89%	91.77%	91.37%	91.91%	91.48%	86.7%	90.45%	77.76%	90.92%	91.73%	92.49%	90.06%	92.45%	92.49%	96.76%

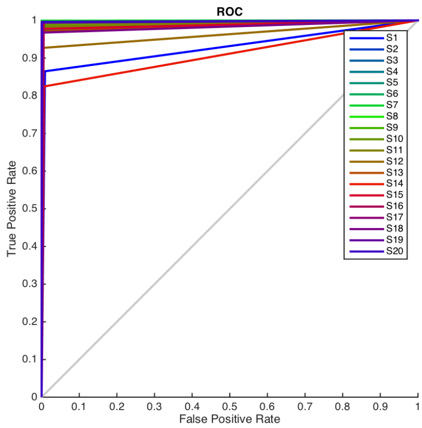

Fig 4.14: ROC figure for NN for channels C3, C4, F3, F4, FC1, FC2, FC5, and FC6

Table 4.28: ROC Area Under Curve for NN for Channels C3, C4, F3, F4, FC1, FC2, FC5, and FC6

Subject	Area	Subject	Area
S1	0.911	S11	0.991
S2	0.996	S12	0.974
S3	0.999	S13	0.99
S4	0.999	S14	0.932
S5	0.994	S15	0.99
S6	0.989	S16	0.945
S7	0.999	S17	0.998
S8	0.993	S18	0.985
S9	0.993	S19	1.0
S10	0.991	S20	0.99
Average			0.98295

4.8 Re-testing Data

Table 4.29: Data After 6 Months

Subject	SVM	NN
S2	93%	80%
S7	95%	85%
S10	72%	67%

Table 4.29 shows the accuracy of the system after 6 months. It shows that the system doesn't change over time; it also shows that NN still gets lower results than the SVM classifier. The data was tested against former data to get the accuracies and uses only 2 channels. S10 got the worst data of all 3, but it's data is still on the average. Meanwhile S7 has the highest accuracy of being right.

4.9 Discussion

Comparing all the averages for the area under the ROC curves for all the different channels, It is seen that the best results overall were for channels C3, C4, FC1, FC2, FC5, and FC6 using the SVM classifier. Also, the NN classifier is prone to have overfitting problems, while the SVM classifier does not.

For some subjects, the SVM presented better accuracy than NN which gave reduced accuracy. This is due to the fact that, the SVM maps the features to a higher dimensional space and fits linear decision boundaries in the high dimensional space. The NN classifier is unreliable as it changes weights from session to session. If a subject has lower accuracy for authentication with both classifiers, this implies that the subject needs more training in performing the motor imagery tasks.

Also, it can be seen that the overall performance was high with an accuracy of 97% with just using 3 electrodes for 20 subject authentication problem. Using only 2 electrodes also gives a good accuracy of 91%. These results indicate that the algorithm can be optimized to work with fewer electrodes by better subject training, improving the feature extraction and feature selection processes.

While the SVM classifier might not be prone to overfitting, it does have a problem with scalability, while it is not in the scope of this project to test that, in theory, is still a problem. Because the SVM uses one-vs-one algorithms to classify, the time to classify would become exponential, while the NN wouldn't. For small systems, SVM is used with 2 channel EEG for authentications in real-time. Next, the chapter presents some results using a GUI and timing results for offline person verification. An authentication system can use only two channels because results weren't that different from the best results, and with the SVM classifier for a limit number of people or using the NN classifier with less sampling.

Chapter 5

OFFLINE GUI

This chapter shows an implemented off-line GUI that can train the NN classifier and the SVM classifier. The GUI is made using a combination of the python and Matlab programming languages. The python code uses the Tkinter library to create the interface and uses a Matlab engine to communicate to be able to use Matlab functions.

Fig 5.1 shows what the user sees when he starts the GUI. The first button is the classifiy button, which allows a user to authenticate aperson data. The Button of Train allows a user to train the NN and the SVM classifier with data preiviously recorded.

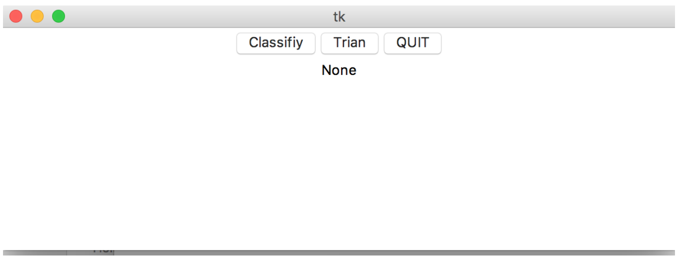

Fig 5.1: ROC figure for NN for channel C3, C4, F3, F4, FC1, FC2, FC5, and FC6

After prassing the Train button, the user sees the image in Fig 5.2 and can select one of the the classifiers to train. Once the slected classifier is trained the GUI shows the word finish as displayed in Fig 5.3, to tell the user that the GUI finished training the selected classifier.

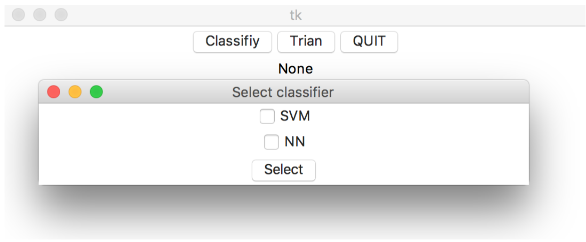

Fig 5.2: Display of Buttons in the GUI

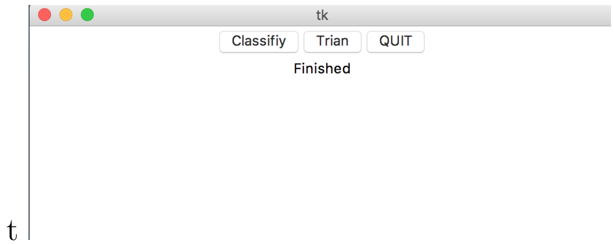

Fig 5.3: Images of GUI displayig the Word Finish after Finishing Classifing

After the user has train the classifier at least once the user can be classified a subject data even if the user closes the app. If the user presses the classify button a pop up similar to Fig 5.2 shows the option of which classifier to choose. After choosing a classifier a popup with a file browser is displayed show in Fig 5.4 after selecting the folder that with the data the user wants to classify, the software classifies it and displays it. Fig 5.5 demostrates the example of using subject 1 data and being classified

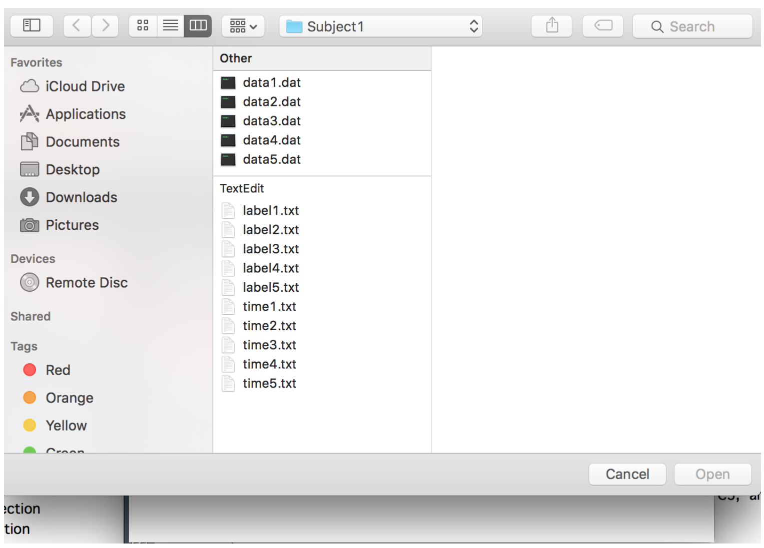

Fig 5.4: Image of file browser for the software.

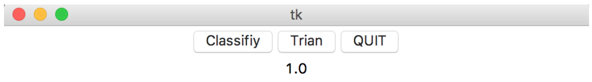

Fig 5.5: Image of data being authenticated as subject 1

Chapter 6

CONCLUSION

6.0.1 Contributions

The spectrogram was used to extract features from EEG signals in experiments based on motor imagery and different channels were tested to see which ones would be more beneficial for person authentication. Because of the methods used here, better results were acquired than previous work for all group of channels tested.

The Support Vector Machine was compared with the Neural Network classifier, the Support Vector Machine has better results for all of the channels. The SVM is more reliable because it doesn't have the overfitting problem which lowered the results for the other channels.

The 2 best EEG channels were C3 and C4, their results were very close to the result with 6 channel. This will decrease the time for set up. While using an SVM classifier might be more reliable for a small authentication system an NN with less training would be a better classifier for a larger neural classification.

6.0.2 Future Work

The EEG based person authentication system presented here could be used to develop an automatic way for person identification, by implementing the system in a smart device, where it would show the outcome of the authentication on the said device[32].

To improve the peresnted methods to classyfiy a person's EEG some sugestions are given below:

- Improving the SVM classifier to allow scalability would allow the system to target a larger population.

- Another option to improve person authentication accuracy will be to explore spectrotemporal and positive matrix factorization methods for feature extraction.
- Using texture desciptros on the EEG data as another feature can improve the accuracy of the system.
- Improve classifier performance by combining SVM and NN classifiers.

Bibliography

[1] Ji, Z., and Qin, S. (2003, April). Detection of eeg basic rhythm feature by using band relative intensity ratio (brir). In Acoustics, Speech, and Signal Processing, 2003. Proceedings.(ICASSP'03). 2003 IEEE International Conference on (Vol. 6, pp. VI-429). IEEE.

[2] R. Palaniappan and D. P. Mandic, EEG based biometric framework for automatic identity verification, Journal of VLSI signal processing, vol. 49, pp. 243-250, 2007.

[3] P. Baekgaard, M. K. Petersen and J. E. Larsen, In the twinkling of an eye: Synchronization of EEG and eye tracking based on blink signatures, Proc. 4th Intl. workshop on cognitive information processing, 2014.

[4] La Rocca, D., Campisi, P., & Scarano, G. (2012, September). EEG biometrics for individual recognition in resting state with closed eyes. In Biometrics Special Interest Group (BIOSIG), 2012 BIOSIG-Proceedings of the International Conference of the (pp. 1-12). IEEE.

[5] Maiorana, E., Sol-Casals, J. & Campisi, P. Machine Vision and Applications (2016). doi:10.1007/s00138-016-0804-4

[6] Maiorana, E., La Rocca, D., & Campisi, P. (2015, June). EEG-based biometric recognition using EigenBrains. In Multimedia & Expo Workshops (ICMEW), 2015 IEEE International Conference on (pp. 1-6). IEEE.

[7] H. A. Shedeed, A new method for person identification in a biometric security system based on brain EEG signal processing,

[8] M. K. Abdullah, K. S. Subari, J. L. C. Loong and N. N. Ahmad, Analysis of effective channel placement for an EEG-based biometric system, Proc. EMBS on Biomedical Engineering and Science, 2010.

[9] S. Marcel and J del R. Milan, Person authentication using brain waves (EEG) and maximum a posteriori model adaptation, IEEE Trans. On PAMI, 29(4), 2007.

[10] R. Palaniappan and D. P. Mandic, Biometrics and brain electrical activity: A machine learning approach, IEEE Trans. PAMI, 29(4), 2007.

[11] R. Palaniappan, Method of identifying individuals using VEP signals and neural networks: IEE Proc. Online number 20040003, 2004.

[12] A. K. Jain, P. Flynn and A. A. Ross, Handbook of biometrics, 2007.

[13] Zhong J.; Shuren Q. Detection of eeg basic rhythm feature by using band relative intensity ratio (brir). ICASSP, VI:429432, Apr 2003.

[14] E. Alpaydin, Kernal Machine, in Introduction to Machine Learning, 3th ed. Cambrige Massachusetts:MIT, 2014, ch. 13, sec. 13.6, pp. 283-284

[15] Chang, C. C., and C. J. Lin. "LIBSVM: A library for support vector machines. 2001.[cited in 2001]." Software Available from: http://www. csie. ntu. edu. tw/ cjlin/libsvm.

[16] T. Guernine. (2011,). New fuzzy multi-class method to train SVM. Presented atThird International Conference onn Advanes in Databases, Knowledge, and Data Applicationn.

[17] Gose, Earl, Richard Johnsonbaugh, and Steve Jost. Pattern Recognition and Image Analysis. Upper Saddle River, NJ: Prentice Hall PTR, 1996. Print, ch 6, sec 6.1-6.4, 227-244 pp

[18] M. K. Abdullah, K. S. Subari, J. L. C. Loong and N. N. Ahmad, Analysis of effective channel placement for an EEG-based biometric system, Proc. EMBS on Biomedical Engineering and Science, 2010.

[19] Hu, J. F. (2009, December). New biometric approach based on motor imagery EEG signals. In BioMedical Information Engineering, 2009. FBIE 2009. International Conference on Future (pp. 94-97).

[20] Mustafa, M., Taib, M. N., Murat, Z. H., Sulaiman, N., and Aris, S. A. M. (2011, March). The analysis of eeg spectrogram image for brainwave balancing application using ann. In Computer Modelling and Simulation (UKSim), 2011 UkSim 13th International Conference on (pp. 64-68). IEEE.

[21] Qiao, Xiaoyan, et al. "Feature extraction and classifier evaluation of EEG for imaginary hand movements." Natural Computation (ICNC), 2010 Sixth International Conference on. Vol. 4. IEEE, 2010.

[22] Kohavi, R. (1995, August). A study of cross-validation and bootstrap for accuracy estimation and model selection. In Ijcai (Vol. 14, No. 2, pp. 1137-1145).

[23] Hsu, Chih-Wei, and Chih-Jen Lin. "A comparison of methods for multiclass support vector machines." Neural Networks, IEEE Transactions on 13.2 (2002): 415-425.

[24] Y. Fang, M. Chen and R. F. Harrison, A multi-class pattern recognition method for motor imagery EEG data, Proc. IEEE intl. conference on systems, man and cybernetics, 2011.

[25] P. Herman, G. Prasad, T. M. McGinnity and D. Coyle, Comparative analysis of spectral approaches to feature extraction for EEG-based motor imagery classification, IEEE trans. Neural systems and rehabilitation engineering, vol. 16, no. 4, 317-326, 2008.

[26] Q. Xu, H. Zhou, Y. Wang and J. Huang, Fuzzy support vector machine for classification of EEG signals using wavelet-based features, Journal of medical engineering & physics, vol. 31, 2009.

[27] Ge S, Wang R, Yu D (2014) Classification of four-class motor imagery employing single-channel electroencephalography. PLoS ONE 9(6): e98019. doi:10.1371/journal.pone.0098019W.-K. Chen, Linear Networks and Systems (Book style). Belmont, CA: Wadsworth, 1993, pp. 123135.

[28] Manian, Vidya, Ramn Vsquez, and Praveen Katiyar. "Texture classification using logical operators." Image Processing, IEEE Transactions on 9.10 (2000): 1693-1703.

[29] J. Whitehill, C.W. Omlin, Haar features for facs au recognition, Proc. 7th intl. conf. on automatic face and gesture recognition, 2006.

[30] M.T. Pham, T.J. Cham Fast training and selection of Haar features using statistics in boosting-based face detection, Computer Vision, 2007.

[31] Marques, Oge. Practical Image and Video Processing Using MATLAB. Hoboken, NJ: Wiley/IEEE, 2011. Print.

[32] Klonovs, J., Petersen, C. K., Olesen, H., and Hammershoj, A. (2013). ID proof on the go: Development of a mobile EEG-based biometric authentication system. Vehicular Technology Magazine, IEEE, 8(1), 81-89.

[33] Zweig, M. H., & Campbell, G. (1993). Receiver-operating characteristic (ROC) plots: a fundamental evaluation tool in clinical medicine. Clinical chemistry, 39(4), 561-577.